Carbonation of cementitious backfill for geological disposal of nuclear waste: Nirex Reference Vault Backfill

Nicholas C Collier[a], David W Heyes[a], Ed J Butcher[a,*], Jason Borwick[a], Antoni E Milodowski[b], Lorraine P Field[b], Simon J Kemp[b], Ian Mounteney[b], Susan A Bernal[c], Claire L Corkhill[c], Neil C Hyatt[c], John L Provis[c], Leon Black[d]

[a] National Nuclear Laboratory, Havelock Rd, Derwent Howe, Workington, CA14 3YQ, UK.

[b] British Geological Survey, Environmental Science Centre, Nicker Hill, Keyworth, Nottingham, NG12 5GG, UK.

[c] NucleUS Immobilisation Science Laboratory, Department of Materials Science and Engineering, The University of Sheffield, Mappin Street, Sheffield, S1 3JD, UK.

[d] School of Civil Engineering, University of Leeds, Woodhouse Lane, Leeds LS2 9JT.

* Corresponding author. Email ed.j.butcher@nnl.co.uk.

Keywords: NRVB, Nirex Reference Vault Backfill, carbon dioxide, carbonation, cement, intermediate level waste, immobilization.

Commented [C1]: Or something like this to describe the work more clearly. No one but a handful of people in the UK know what on earth NRVB is…

Abstract

The ability of Nirex Reference Vault Backfill (NRVB), a cement backfill material, to ~~remove~~ capture carbon dioxide from I~~i~~ntermediate L~~l~~evel R~~r~~adioactive waste packages after repository backfilling, has been assessed. Large-scale trials assessed the physical and chemical reaction of carbon dioxide with the hardened backfill grout. A carbonation front, radial in nature, was observed extending in~~-~~to the grout and ~~-~~ T~~t~~hree distinct regions were identified in the hardened grouts. A ~~carbonated, partially carbonated and uncarbonated. Within the~~ partially carbonated region, a carbonation front, and a transition zone were discerned. Potassium, and to a lesser extent sodium, ~~are~~ were concentrated ~~within a zone~~ in the carbonated region just ahead of the main reaction front. The area just ahead of the carbonation front wa~~i~~s enriched in both sulphur and aluminium, while sulphur ~~is~~ was found to be ~~then~~ depleted from the carbonated material behind the main reaction front indicating that???. ~~SEP~~Within the main carbonated region, virtually all of the hydrated cement phases ~~are~~ were found to be carbonated, and carbonation extended throughout the ~~.~~ ~~Some carbonation had occurred throughout the canister~~grout, even within material indicated by phenolphthalein solution to be uncarbonated. Importantly, since the cement backfill relies upon its high porosity to fulfill its groundwater buffering function, carbonation was found to significantly impact the porosity of the cement; in the carbonated region the porosity was significantly reduced, while in the partially carbonated region it was increased.

~~The porosity of the carbonated grout is lower than in the uncarbonated material due to replacement of pore space with precipitated calcium carbonate, but the highest porosity was measured in the partially carbonated region.~~SEP

Commented [C2]: If this is going to be REF returnable, it needs to say something about "so what?".

Commented [C3]: What is the scientific significance of this?

Commented [LB4]: ?

Commented [NC5]: JP Issue.

Commented [LB6R5]: I think that this has been addressed. It is known that phenolphthalein can underestimate the depth of carbonation, and calcium carbonate enveloping portlandite (as seen in figure 9) is known to cause this.

1. Introduction

Geological disposal in an engineered facility underground is the preferred option for disposal of nuclear waste. ~~A range of generic disposal concepts for High Level Waste (HLW), spent fuel (SF) and Intermediate and some Low Level Waste (ILW/LLW) streams are being considered in the UK~~ [Nuclear Decommissioning Authority, 2010a]. Such ~~Geological~~ geological disposal facilities (GDFs) are based on ~~concepts, also known as Geological Disposal Facilities (GDFs), have been selected based on three host rock types (higher strength rock, lower strength sedimentary rock and evaporites). All these concepts~~ the of use a multi barrier containment approach, which involves the application of engineered barriers, ~~that would~~ working in combination with natural geological features, to reduce the rate of radionuclide release to the biosphere. ~~and delay ultimate return to the surface environment.~~ In the United Kingdom, for the disposal of Intermediate Level Waste (ILW) ~~/LLW~~ in a higher strength rock, it is proposed that packages of grouted waste ~~are proposed to~~will be emplaced in sub-surface vaults and surrounded with a Portland cement-based backfill called Nirex Reference Vault Backfill (NRVB)[Vasconcelos et al. 2018]. The primary advantages of using this material are: i) ~~One of the main reasons cementitious grout is being considered for waste encapsulation and back-filling, is~~ its ability to maintain highly alkaline pore solutions, which ~~. This~~ reduces the solubility and mobility of many of the important radionuclides, thereby ~~restricting~~ retarding their migration from the GDF and into the geosphere; ~~. It also inhibits and slows the corrosion of the steel waste canister~~ii) its high porosity and ~~,~~ ~~The NRVB is not a structural cement; in addition to providing a chemical conditioning function, the NRVB is specifically formulated to be~~ gas-permeability, which give a high surface area for radionuclide sorption and allows relief of any pressure from gas egress from the waste packages; iii) its low strength, which ~~le and to be weak enough to be~~supports easy ~~ily~~ excavat~~ed~~ion of waste packages, if required; and iv) it also inhibits and slows the corrosion of the steel waste canister. ~~in the event of the need for waste recovery.~~

~~It is expected that some of the wastes in a GDF would produce gaseous emissions~~ T~~[Nuclear Decommissioning Authority, 2010b]~~, ~~t~~he bulk of gaseous emissions from ILW packages ~~which will~~are expected to be hydrogen (H_2), mainly produced from the corrosion of metallic waste products~~.~~ and m~~M~~ethane (CH_4) and carbon dioxide

Commented [C7]: Please add Rita's new paper here: Vasconcelos R. G. W., Beaudoin N., Hamilton A., Hyatt N. C., Provis J. L. and Corkhill C. L. Characterisation of a high pH cement backfill for the geological disposal of nuclear waste: The Nirex Reference Vault Backfill. Applied Geochemistry, 89, 180 – 189 (2018).

Commented [NC8]: Added by Tony.

Formatted: Highlight

Formatted: Highlight

Formatted: Highlight

Formatted: Highlight

Formatted: Highlight

Formatted: Highlight

Commented [AM9]: Added this statement to provide relevant introductory information: it is relevant to why the NRVB has its specific formulation.

Formatted: Highlight

Formatted: Highlight

Commented [NC10]: Use more recent reports Tony has identified?

(CO_2), ~~are also likely to be~~ produced *via* the microbial degradation of organic waste materials under ~~aerobic~~ anaerobic or aerobic~~anaerobic~~ conditions [Nuclear Decommissioning Authority, 2010b]. A small proportion of the gas produced ~~would be radioactive which~~ would include radioactive tritium (^3H), ^{14}C- labeled species (including $^{14}CH_4$ and $^{14}CO_2$) and radon (Ra). ~~After backfilling, and before and after the subsequent closure of the vaults, i~~It is desired that, after backfilling, either the cementitious material in the waste packages, or in the backfill, would capture ~~-~~any waste CO_2 ~~generated *in situ* within the grouted waste packages~~ (including $^{14}CO_2$) ~~would~~, thus preventing its egress to the geosphere. ~~react fully with either the ILW/LLW encapsulation grouts or the cementitious backfill by carbonation of cationic species, and so would be removed from the gaseous phase and retained in either the engineered barrier system, the encapsulation grouts, or the backfill, or the engineered barrier system,~~

~~Carbon dioxide is known to react with cementitious materials in a process known as carbonation [Basheer *et al.*, 2001; Hobbs, 2001; Poonguzhali *et al.*, 2008]. While this may be a durability concern for reinforced concrete, it may also confer benefits, for example reduced porosity and so improved durability of in fact, deliberate carbonation of pre-cast concrete members or, in the case of NRVB, sequestration of carbon dioxide can be used as a means of improving durability. This process is controlled by the movement of gaseous CO_2 into the material, driven by concentration and/or pressure gradients, and its chemical reaction with calcium-rich phases present in the binding phase. The extent of carbonation is controlled by the chemistry and permeability of the cement. The main effect of carbonation in Portland cement-based binders is a reduction in the alkalinity of the material, along with a possible variation in mechanical strength, and alteration in permeability of the binder [Bary and Sellier, 2001; Basheer *et al.*, 2001; Fernández-Bertos *et al.*, 2004; Morandeau *et al.*, 2014]. The combined effect of the changes induced by carbonation in a cement grout can be detrimental, as the presence of a highly alkaline pore solution is one of the main criteria used to determine the life-span of the UK geological disposal repository concept for radioactive wastes [Atkins and Glasser, 1992]. Such conditions reduce the solubility and enhance the sorption of many radionuclides, which restricts retards their release from the cement and the repository into the geo- and bio-spheres.**

Formatted: Font: Italic

Commented [EJB11]: Changed so that the order is consistent with the gases being produced – CH4 from anaerobic

Commented [NC12]: Use more recent reports Tony has identified?

Formatted: Font: Italic

Commented [EJB13]: Changed for logic – starting with the inner most grout and working outwards

Commented [C14]: Repeated from above – no need to mention again

Formatted: Font: (Default) Times New Roman, Font color: Auto

~~The carbonation of cementitious materials has been studied widely in the construction industry because of its effects on the performance of reinforced concrete engineering structures exposed to atmospheric CO_2 [Thiery *et al.*, 2007; Black *et al.*, 2008].~~ In ordinary Portland cements used for construction purposes, CO_2 from the atmosphere diffuses through gas-filled pores and dissolves into the pore solution ~~to~~ forming aqueous HCO_3^-. The uptake of acidic CO_2 into the alkaline pore solution reduces the internal pH of the binder, and the dissolved carbonate also reacts with calcium-rich hydration products present in the matrix, mainly with portlandite ($Ca(OH)_2$), calcium silicate hydrate (C-S-H[1]) and the various calcium aluminate hydrates present, to form solid calcium carbonates, silica gel and hydrated aluminium and iron oxides [Johannesson and Utgenannt, 2001; Živica and Bajza, 2001; Fernández-Bertos *et al.*, 2004].

The effect of carbonation on the ability of a cementitous backfill grout to buffer groundwater to high pH (as desired to retard release of radionuclides to the geosphere) has not been fully elucidated. ~~In addition, carbonation of the cement grout reduces the ability of the cement to buffer the pore waters to high pH, which is one of the main geochemical functions of the cement within the engineered barrier system.~~ The reaction of CO_2 with typical waste encapsulation grouts and NRVB has been studied [Harris *et al.*, 2003a; Harris *et al.*, 2003b; Sun, 2010], but further information is required to enable a safety case for disposal to be put forward on firm scientific foundations.

We report here on ~~full~~ detailed ~~larger scale~~ experimental studies investigating the reaction of gaseous CO_2 with hardened NRVB grout to support understanding of ~~determine the likely interactions between the CO_2 wastes and~~ the backfill material following closure of the GDF. ~~The trials provided new insight into the reaction of CO_2 with hardened NRVB grout, m~~Making use of chemical and microstructural analyses, we show that ….. [need to put conclusions here].~~high resolution analytical tools to provide an unprecedented level of insight into the carbonation process of NRVB, and its implications for the material in service.~~

[1] Calcium silicate hydrate is the principal binding phase in Portland cement based systems. C, S and H indicate the oxides of calcium, silicon and hydrogen respectively, while the hyphens reflect the variable composition of the material.

Commented [LB15]: Don't think that this reference is relevant.

Commented [EJB16]: Happy enough for this to be removed

Commented [EJB17]: Doesn't this repeat the statement that's in line 102-107 above?

Formatted: Font: (Default) Times New Roman, Font color: Auto

Commented [EJB18]: Changed because RWM were clear in their comments on the original report that we are not simulating a GDF

Commented [C19]: Sometimes this is called grout, other times backfill. Need to pick one and be consistent throughout.

Formatted: Highlight

Formatted: Highlight

Formatted: Font: (Default) Times New Roman,

Formatted: English (United Kingdom)

2. Experimental

2.1 Materials

Nirex Reference Vault Backfill (~~The~~ NRVB) was formulated according to [ref] using Ribblesdale Sellafield specification ~~powders consisted of:~~

- ~~Ordinary~~ Portland Cement ~~(~~ ~~Sellafield Ltd specification ordinary Portland cement, supplied by~~ Hanson Cement~~), ex Ribblesdale works~~ [Cann and Orr, 2010]~~. l. This cement is developed specifically for the UK nuclear waste processing industry and is different from cements used in construction, in that it does not contain calcium carbonate and is ground without the use of organic grinding agents.~~
- ~~L~~imestone flour ~~(~~ ~~supplied by~~ Tendley Quarries ~~to BS594-1~~ [BS594-1, 2005]) and h~~.~~
- ~~H~~ydrated lime ~~(~~ Limbux hydrated lime supplied by Tarmac Buxton Lime and Cement [BS EN 459-1, 2015]). Characterisation of each of these materials (e.g. particle size, surface area, composition etc. are provided in Vasconcelos et al. (2018)).

The formulation of the NRVB paste is shown in Table 1; the overall water to ~~:~~solids ratio (w/~~:~~s) was 0.55.

Table 1. NRVB composition [Francis *et al.*, 1997]

Components	Mass (g)	Paste Proportion (wt.%)	Solids Proportion (wt.%)
Ordinary Portland cement	450	26.01	40.36
Limestone flour	495	28.61	44.39
Hydrated lime	170	9.83	15.25

Formatted: Normal, No bullets or numbering

Water		615	35.55	-
	Total	1,730	100	100

2.2 Large-scale trial

Powders sufficient to produce a 500 L batch of grout were weighed and then added to the desired weight of water at a controlled rate over a 25 minute period into a BNFL grout mixer (an impeller in ~~-~~vessel mixer, as used in the Sellafield Wastes Encapsulation plant (WEP)) and then mixed for a further 15 minutes. The grout was ~~then~~ poured into a bespoke 400 L stainless steel curing vessel (Figure 1). The vessel had an internal diameter of 790 mm, an internal height of 780 mm, and incorporated a stainless steel ILW drum lid (with a standard sintered metal vent at the centre of the lid) fixed inside. A sealed compartment located directly below the vent provided a gas-tight reservoir from which the CO_2 was emitted. Before the 400L vessel was filled with grout, the inside faces were roughened. ~~and coated with an~~After filling with the NRVB, the ~~edge~~ interface between the top surface of the NRVB and the vessel was filled with a beading of ~~-~~epoxy resin-based concrete bonding material to ensure good adhesion between the grout and the walls of the vessel (and hence reduce the pathways available for the CO_2 to flow around the grout). The vessel was then filled with 302 L of grout to cover the drum vent and form an interface with the drum lid; this simulated the backfilling of a GDF vault filled with ILW containers. The sample was sealed and ~~then~~ cured at 40°C for 28 days to ~~mimic~~ represent potential repository conditions. After this period the internal gas reservoirs were filled with CO_2 (99.8 % purity) to 0.15 MPa from an external gas bottle through a ~~penetration~~ connection in the base of the vessel and into the reservoir. CO_2 pressure was measured at the gas inlet reservoir throughout, and gas consumption was calculated from pressure changes. The carbonation trial was performed at 30°C and autogenous RH~~;~~ ~~and~~ temperature and pressure were recorded for the duration. The vessel was fitted with a carbon dioxide sensor in the external lid of the 400 L vessel to detect any release of CO_2 from the top surface of the grout, which would indicate either premature material failure, *e.g.* by cracking, or CO_2 permeation ~~of~~ through the whole depth of the grout ~~by the CO_2~~.

Commented [LB20]: Can we give a justification for this? I think that it's valid, but if you get a pedantic review they will query whether the conditions are appropriate.

Would you expect high CO2 concentrations in an encapsulation matrix?

Commented [EJB21]: Leon – I'm not sure we can, given the uncertainties about the waste the pressure was selected to give sufficient driving force to expel the CO2, but wasn't a comprehensive representation of what the conditions in waste packages are,

Formatted: Subscript

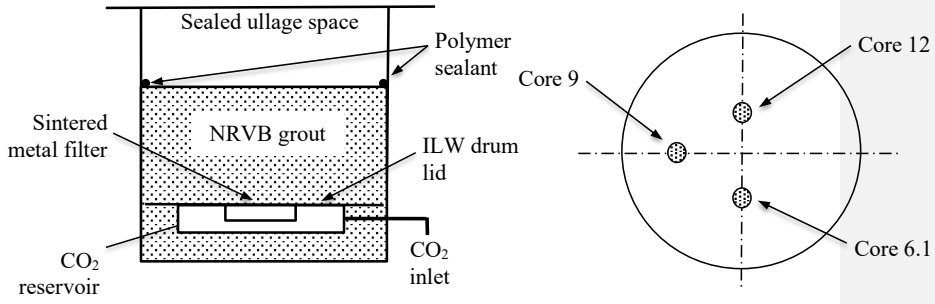

Figure 1. ~~The s~~Schematic ~~shows of~~ the ~~layout of the~~ large-scale trial equipment layout and a plan view of core locations. ~~showing the location of the cores taken~~

After approximately 2 years of curing and exposure to CO_2, the trial was terminated and three 48 mm diameter cores were drilled perpendicularly to the top surface and through the full thickness of the grout until the embedded steel ILW drum lid was reached~~. Three cores were taken (, and their positions and locations varied were as shown in~~ Fig~~ure~~. 1). ~~The radial distance from the centre of the vessel to the centre of both Core 6.1 and Core 12 was 100 mm, whereas that of Core 9 was 150 mm.~~ Water was used minimally for cooling and lubrication fluid during the drilling process. After removal, each core was placed and sealed in an argon-purged polythene sleeve ~~that had previously been purged and filled with technical grade argon~~, and then double bagged in a second polythene sleeve. After coring, samples were sprayed with a solution of 0.2% phenolphthalein in denatured ethanol, and photographed to allow areas of bulk carbonation to be visually identified.

2.3 Carbon dioxide uptake and depth of carbonation

The maximum depth of carbonation at the single exposed face of the large-scale trials was calculated using information on the maximum measured carbonation extent of small NRVB cubes exposed to a 99.8% CO_2 gas environment until equilibrium [Heyes *et al.*, 2015], 6200 (±400) mol CO_2/m^3 NRVB. This calculation is explained in detail in the Supplementary Material.

Commented [C22]: Can't we just call the cores "1, 2 and 3" throughout? Makes no difference to the reader what the actual names are, in fact, simplifying this makes it easier to read. You could always list the actual sample names in the supplementary material?

Formatted: Subscript

Commented [C23]: Do we really need that information?

2.4 Analytical methods

Information describing the details of the techniques used is included in Supplementary Material, but brief summaries are given here. Thermogravimetric Analysis (TGA) and Differential Scanning Calorimetry (DSC) were performed using a Netzsch STA409PC Simultaneous Thermal Analyser, using ~30 mg samples in a nitrogen atmosphere, heated from 50 to 1000°C at 10°C/min. For permeability testing, a Temco MP-402 'mini'- or 'probe-permeameter' was used. Measurements were made on the cut flat face of one half of the intact cement cores in a horizontal orientation. Flow rate and pressure were recorded and permeability was calculated. Measurements were repeated several times at the same spot and the mean was taken as the representative permeability. Measurements were recorded at various points along the length of each core at intervals of ~10 – 20 mm apart.

Formatted: English (United States)

Selected thin sections of each sample were carbon coated (~25 nm layer) and then examined using backscattered scanning electron imaging (BSEM) and energy-dispersive X-ray microanalysis (EDXA) elemental mapping. This was performed using an FEI QUANTA 600 environmental scanning electron microscope (ESEM) equipped with an Oxford Instruments INCA Energy 450 EDXA system. Semi-quantitative EDXA point analyses were recorded from selected X-ray mapped areas to aid phase differentiation and identification, and processed using the inbuilt "standardless" calibration Oxford Energy INCA Suite Version 4.15 (2009) software package.

Formatted: Highlight

Laser ablation-inductively coupled-mass spectroscopy (LA-ICP-MS) was performed using an Agilent 4500 ICP-MS, combined with a laser ablation function, on 1 mm thick samples. X-ray microtomography measurements were carried out using a Nikon Metris Custom Bay instrument, and porosity was calculated by thresholding and segmentation of the reconstructed data [Provis *et al.*, 2012]. Raman and Fourier Transform Infra-Red (FTIR) spectroscopy were both used to study material either side of a visible carbonation front. Raman spectra were recorded using a Renishaw System 2000 Raman spectrometer fitted with an Ar^{+} laser (514.5 nm). Twenty spectra were

Formatted: Superscript

accumulated, with a 10 second acquisition time, typically over the wavenumber range 200 to 1200 cm^{-1}, and samples were left under the laser light for up to 20 minutes prior to collection of the spectra to "photobleach" and reduce fluorescence. ~~For FTIR analysis, mid-IR images were collected using a Varian 680-IR FT-IR spectrometer fitted with a 64 x 64 mercury-cadmium-telluride focal plane array detector. Three images were measured in transflection mode (FoV 350 x 350 µm) using a spectral resolution of 8 cm^{-1}, an integration time of 0.025 and 512 co-additions. Images were taken either side of, and directly on, the transition zone.~~ For X-ray diffraction (XRD), samples were finely-ground ~~micronised~~ under acetone with 10% corundum (Al_2O_3) as an internal reference to allow validation of quantification results. XRD was carried out using a PANalytical X'Pert Pro series diffractometer equipped with a cobalt target tube, X-Celerator detector and operated at 45 kV and 40 mA. The ~~micronized~~ powder samples were scanned from 4.5 - 85° 2θ at a scan rate of 2.76° 2θ/minute. Quantification was achieved using the Rietveld refinement technique (*e.g.* Snyder and Bish [1989]) using PANalytical HighScore Plus software together with the latest version of the International Crystal Structure Database (ICSD).

Commented [LB24]: This can be deleted since FTIR data is no longer being included.

Commented [AM25]: Delete "micronised". And replace by "finely-ground". This should make it cleare for those unfamiliar with the term "micronized"

Formatted: Highlight

Formatted: Strikethrough

3. Results and Discussion

3.1 Carbonation front and visual characteristics

Visual analysis of the phenolphthalein staining ~~in the large-scale samples~~ demonstrated that carbonation ~~does not proceed via a horizontal reaction front progressing in a direction parallel to the horizontal surface of the sample, but actually~~ progresse~~s~~d radially from the vent ~~because of the point source of CO_2~~. ~~However,~~ ~~p~~Phenolphthalein staining showed no evidence to suggest that gas travelled along the drum lid interface and/or up the side of the vessels, suggesting a good circumferential seal between the grout and the container.

~~Phenolphthalein staining does not reveal the precise location of a carbonation front, but it does show where complete carbonation has occurred.~~ Phenolphthalein staining (later confirmed by micro-focus techniques) was used to identify three distinct regions within each core of hardened NRVB grout: ~~(~~i) ~~the~~ uncarbonated ~~region~~; ~~(~~ii) ~~the~~

partially carbonated; ~~region,~~ and~~;~~ ~~(~~iii) ~~the~~ carbonated regions. The partially carbonated region was observed as a distinct interface between uncarbonated and carbonated material, and was likely to be where a carbonation front was located; these three regions are each analysed in detail below. For each core, the assignment of uncarbonated, partially carbonated and carbonated regions was made based on the results obtained using phenolphthalein staining. Phenolphthalein staining was also used to measure the depth of carbonation in each of the three cores~~;, and~~ the average depth was measured to be 26.8 mm, 21.5 mm and 11.8 mm for Core 6.1, 12 and 9, respectively (these were obtained ~~over~~ by ~~average~~ averaging~~readings of~~ between 6 and 8 measurements each).

3.2 Micropermeametry

The permeability, ~~results of micropermeability analyses~~ measured along longitudinal profiles through the three cores, ~~are shown in Table 2, and~~ varied between 0.12 and 1.07 mD (Table 2). These values ~~are~~ were close to the lower limit of detection of the ~~permeabilities that can be measured by the micropermeameter~~ instrument, thus ~~and~~ it was difficult to identify any distinct trends. However, a number of observations could be made. The permeability of ~~the majority of~~ the uncarbonated cement varied mostly between 0.12 and 0.26 mD. No relationship was observed between permeability and distance along the core, other ~~that~~ than in the bottom 1-2 cm of each core (within the carbonation zones) where it was significantly higher, particularly for ~~samples~~ cores 6.1 and 9. Not only did the carbonation cause an increase in the permeability, but the texture of the grout was observed to become "chalky" in all carbonated zones.

Commented [C26]: Yup, "Cores 1 and 2" would be much nicer to use here!

Commented [C27]: Do you mean crumbly? Not sure what else chalky could mean.

Commented [LB28]: This runs counter to prevailing wisdom which says that carbonation lead to a decrease in capillary porosity, (Ngala & Page, CCR, 1997). Now, with a high CO2 concentration from a localized source, the effect on microstructure may be different, hence the increase in porosity.

Having said this, I've looked at the permeability data in the table and there isn't an increase in permeability. In cores 12 and 9 there is a decrease in permeability after carbonation. (You can't take the bottom value which is clearly an outlier).

Commented [EJB29]: Agree – looking at the data, aside from the very bottom of the cores the permeabilities (carbonated/uncarbonated) look to be very similar

Table 2. Micropermeametry results

Vertical Position[a] (cm)	Intrinsic permeability (mD)		
	Core 6.1	Core 12	Core 9
1 (top)	0.24	0.19	0.23
3	0.21	0.12	0.22
5	0.18	0.26	0.21
7	0.18	0.12	0.20
9	0.16	0.14	0.19
10-11	0.17	0.15	0.21
12-13	0.15	0.22	0.21
14-15	0.16	0.23	0.23
15-16	0.18	0.26	0.20
17-18	0.24	0.26	0.20
19-20	0.23	0.12	0.20
21-22	0.20	0.20	0.21
23-24	0.20	0.15	0.24
25-27	0.17	-	0.23
27-29	0.22	0.18	0.15
29-31	0.23	0.14	0.20
31-33	0.21	0.19	0.17
33-36	0.24	0.13	0.18
34-36	0.17	0.20	0.18
36-39	0.16	0.20	0.17
39-40	0.16	0.19	0.19
40-41	0.17	0.18	0.17
41-42	0.15	0.20	0.19
42-43	0.78	0.19	0.17
43-44	0.72	0.26	0.19
44 (bottom)			1.07

Notes. [a] – from top surface of core. The shaded values represent the depth of carbonation indicated by phenolphthalein solution (as reported in section 3.1).

Commented [AM30]: Would it be better to stick to SI units (mm or m) throughout the rather than cm in this table?

Formatted: Highlight

Commented [C31]: Core 1, Core 2, Core 3 perhaps?

Commented [AM32]: Confusing – am I reading this wrong? Please check this is correct in the table – the shaded area shown in this compiled table seems to be inconsistent with the depths of carbonation stated as *"26.8, 21.5 and 11.8 mm for Core 6.1, 12 and 9 respectively"* in Section 3.1. You may want to think about presenting or illustrating this slightly differently!

As shown by the shading in this table in comparison to the depth indicated in the "vertical position" column, it appears to read as if the depth of carbonation is up to 28, 22 and 4 centimeters, in cores 6.1, 12 and 9, respectively

Commented [LB33R32]: Agree. The vertical position must be in mm, surely

Commented [EJB34]: Agree these must be in mm – see Table 6 (page 43) of the NNL 13296 report , which I've sent a link to.

3.3 Acid digestion and LA-ICP/MS

The chemical profile of the cores ~~Very similar LA-ICP/MS~~were similar irrespective of the core analyzed, therefore~~ results were obtained for each of the cores, so the results described here are~~ representative results from both are discussed herein. ~~of each, and it is important to analyse these results based on an understanding of the total compositional profiles of the samples. For this reason, t~~The total elemental concentration~~s of all elements other than Ca~~ determined by acid digestion ~~of each of the sub-samples taken from each identified region~~ are shown in Figure 2 (Ca is not shown here due to the very high concentration of ~3 x 10^5 ppm). ~~By far the major element in each of the carbonated, partially carbonated and uncarbonated regions was Ca, the concentration of which was of the order of ~ $3x10^5$ ppm in each of these three regions. This was at least 1 order of magnitude greater than any of the other elements, and so to aid analysis of the other elements present, the Ca data were excluded from Figure 2.~~ The concentrations of Al, Fe, Mg and Si ~~are~~ were ~~very~~ similar in each of the region~~s~~, indicating that if ~~they~~ migrate~~ion~~ of these elements occurs during carbonation, it is likely to be only over short distances, as shown below.~~; the behavior of these elements immediately around the carbonation front does show subtle yet important changes which will be addressed below.~~ Compared to the uncarbonated region, the carbonated and partially carbonated regions appeared to be relatively enriched in Na and K, and the carbonated region was depleted in S.

~~Important trends were also observed in the minor element distributions, Figure 2b.~~ The concentrations of Sr and Ni were higher in the carbonated region than in the uncarbonated material (although this was a small difference for Sr, Fig. 2). The Ni concentration ~~is~~ was ~~very low overall, but was high~~greatest in the carbonated ~~sample~~region; ~~; this may be because the Ni present is likely to be sorbed on to the C-S-H~~Ni sorbed to C-S-H may be~~, and will be~~ released during carbonation of this phase; Ni has been reported to show very limited incorporation into calcite [Hoffmann and Stipp, 1998]. The elevated concentration of Sr in the carbonated region is likely to be due to co-precipitation with Ca and incorporation (by solid-solution) in $CaCO_3$, which is precipitated in pores during the carbonation reaction [Shafique *et al.*, 1998]. The concentration of metals is also likely to be higher in pore space filled with secondarily precipitated $CaCO_3$ [Lange *et al.*, 1997]. Within error ~~There~~ there was no ~~little if any~~

Commented [C35]: I'm afraid this all so horribly repetitive! Would suggest a new format to make the story so very much clearer (i.e. don't structure by technique). It could look like this: results section (1): chemical changes as a function of carbonation; results section (2) microstructural changes. Then a discussion to bring it all together.

Formatted: Superscript

Commented [NC36]: Tony comment. Petrographic studies here and elsewhere suggest these do probably react with CO2

Commented [EJB37]: We're going to need a phone discussion on this – I could see that if we are freeing up water during the carbonation reaction and pushing the soluble Na and K ahead of the reaction front, the uncarbonated would be enriched in Na/K but I can't see why the carbonated zone is.

Commented [LB38]: I can understand depletion upon carbonation, since the Sulphur could be displaced by the carbonate. But how do you get elemental enrichment? unless the CO2 contains K and Na there is no means of getting these elements into the system.

Commented [LB39R38]: I think that the key must lie in the definition of the carbonation front being that shown by phenolphthalein. Now we've shown that there is carbonation ahead of the phenolphthalein front, then this becomes more feasible. Text should reflect that, by carbonated, we mean regions which are colourless when sprayed with phenolphthalein.

Commented [EJB40]: Agree with Leon's comments on the definition of carbonated (as shown using phenolphthalein)

difference in the concentration of the other minor and trace elements (Ba, Cr, Cu, Mn, Ti, V, Zn and Zr) between each region.

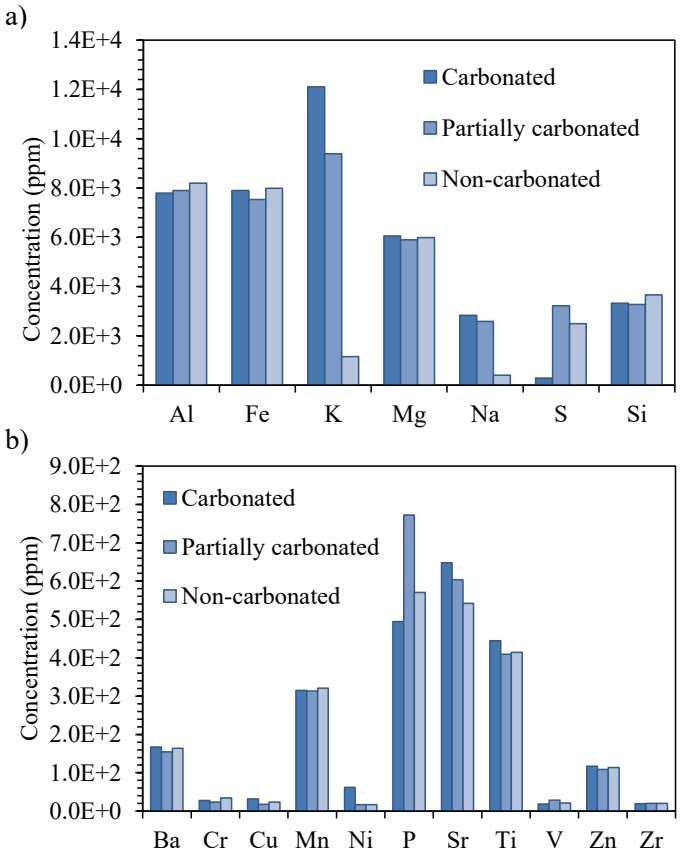

Figure 2. The charts show the elemental concentrations of (a) the major (excluding Ca, at ~3 x 10^5 ppm in all regions) and (b) the minor elements identified in the carbonated, partially carbonated and uncarbonated regions. The errors reported relate to ~~are due to an~~the ICP-MS instrumental uncertainty (2.5%).

Formatted: Centered

Figure 3 shows LA-ICP-MS maps across the carbonated regions in Core 6.1. ~~Figure 3 shows the presence of t~~Two distinct regions with differing chemical compositions were observed: ~~associated with carbonation;~~ one at the reaction front (the carbonation

front) and the other ~~another region just~~ behind the carbonation front (the transition zone), indicating that carbonation did not occur in ~~is not~~ a ~~simple~~ single-step process ~~that occurs~~ at a well-defined single front. The carbonated region was depleted in Ca due to its release from C-S-H during the carbonation process [Morandeau *et al.*, 2014]) and was rich in Si; the decalcification of C-S-H is known to result in the formation of a highly-polymerised Si-rich gel [Fernández-Bertos *et al.*, 2004]. Both Ca and Si were depleted within the transition zone. The contents of Fe and Mg were similar in both the carbonated and uncarbonated regions, but both these elements were slightly depleted in the transition zone, which corresponds to the results obtained by acid digestion (Figure 2a). It is not immediately obvious from thermodynamic or solubility arguments why this should be the case, but this is a point worthy of further investigation in the future.

The most striking difference between regions of carbonated and non-carbonated NRVB shown in Figure 9 wa~~i~~s the distribution of S~~.~~, which was either depleted (carbonated region), low (non-carbonated region) or enriched (carbonation front). ~~The carbonated region was completely depleted in S, the non-carbonated region had a low S concentration, while the carbonation front was enriched in S compared to either of the other regions.~~ This is also reflected in the concentrations of S ~~found following~~measured after acid digestion ~~of each of the samples investigated~~ (Fig~~ure~~ 2)~~.; and the S concentrations in the carbonated, partially carbonated and uncarbonated regions were 280, 3220 and 2500 ppm respectively. This phenomenon may be because~~A ~~a~~ny S present is likely to exist ~~be present~~ in calcium aluminate hydrate phases ~~(,~~ particularly ettringite ~~(see section 3.7)~~ and ~~maybe also~~ AFm~~-~~), which have ~~phases. These phases have~~ low solubility at high pH but are unstable under lower pH conditions, such as those prevalent during carbonation (pH 7 – 8.5) [Morandeau *et al.*, 2014]. Therefore, any S ~~is~~ present would likely ~~to~~ dissolve upon carbonation, and migrate away from the carbonated region towards uncarbonated material ~~before the carbonation front~~. This same phenomenon was observed for ~~appears to occur with~~ Al, where the ~~high~~ elevated concentration of Al ~~concentration~~ before the carbonation front ~~again suggest~~supports the hypothesis that ~~s the decomposition of~~ ettringite or AFm phases decompose upon carbonation and -Al ~~the~~ migrat~~ion~~es towards the ~~of Al to~~ uncarbonated material [Nishikawa *et al.*, 1992]. It is possible that other oxyanions, such as PO_4^{3-}, which are present in the calcium silicate phases of Portland clinker and

Commented [LB41]: This doesn't make sense. Ca will be depleted only because of the presence of additional carbonates. But this will lead to depletion of all elements.

This is suggesting that the Ca/Si ratio of the carbonated paste is lower than in the non-carbonated paste.

It also implies that there's movement of the calcium from the carbonated region

Commented [EJB42]: I agree with Leon concerning the Ca depletion. I can't see how the Ca is going to migrate. Is the reduction in the apparent Ca concentration a function of adding carbonate into the system and the instrumental technique such that the RELATIVE amount of Ca per unit are is decreased? Again worth a phone discussion.

Commented [C43]: Do you mean Figure 3 or 4?

interlayers of C-S-H [Poulsen *et al*. 2010], may undergo a similar process, as evidenced by ~~leading to~~ the apparent enrichment of P in the partially carbonated ~~samples~~ region and depletion in the carbonated ~~samples~~ region, shown in Figure 3.

~~The differences in the elemental concentrations identified between the partially carbonated region and the carbonated and uncarbonated regions of NRVB were investigated further by studying the spatial distribution of specific elements in the partially carbonated region by LA-ICP-MS; the elemental maps for Ca, Si, Al, S, Mg and Fe in this region are shown for Core 6.1 in Figure 3. The results for the other cores were consistent with the data presented here.~~

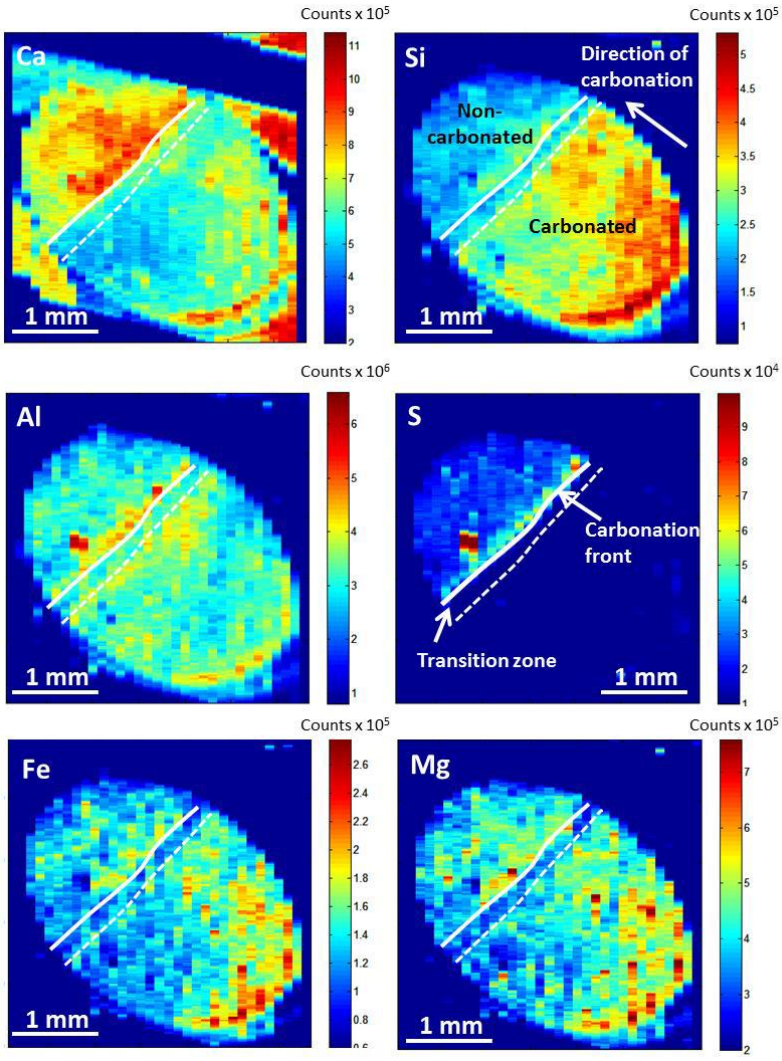

Figure 3. LA-ICP-MS maps showing the relative ~~The figures show the~~ distribution of Ca, Si, Al, S, Fe and Mg in the partially carbonated region of Core 6.1.

Further elemental maps (Fig. 4) were acquired on a duplicate sample, taken from a region ~~which~~ that was also measured using X-ray microtomography (see below)~~, see Section 3.4~~. ~~Figure 4 shows the resulting elemental distributions of Ca, Si, Al, and S, in addition to the alkali elements Na and K.~~ In agreement with the data presented in

Figure 3, this sample also demonstrated a carbonation reaction front, however the determination of its location and the analysis of a transition zone was hampered by the presence of an unreacted particle of cement at the carbonation front (see Si, Al and S elemental maps, Figure 4) and also by the presence of a crack (see Si, Na and K elemental maps, Figure 4).

The distributions of elements ~~Ca, Si, Al and S in Figure 4 appear to be~~were broadly consistent with those observed in Figure 3, giving further evidence for the decalcification of C-S-H in carbonated regions.

In agreement with the digest data for Na and K (Fig. 2), ~~, but not yet full carbonation of an Al-rich ettringite or AFm phase ahead of the carbonation front.~~ these elements were observed to be ~~The acid-digestion concentrations of Na and K were significantly different in the non-carbonated region from the partially carbonated and carbonated regions (Figure 2), indicating an enrichment of the alkali elements in the carbonated region. This is consistent with the elemental maps shown in Figure 4, where both Na and K are~~ enriched in the carbonated region and depleted in the non-carbonated region. T~~Furthermore, t~~he ~~distribution~~ concentration of ~~both~~ Na and K was lower in the vicinity of the front~~:. The~~ the implications of these observations will be explored in more detail in Section 4.

478
479
480
481
482
483
484
485
486
487
488
489
490

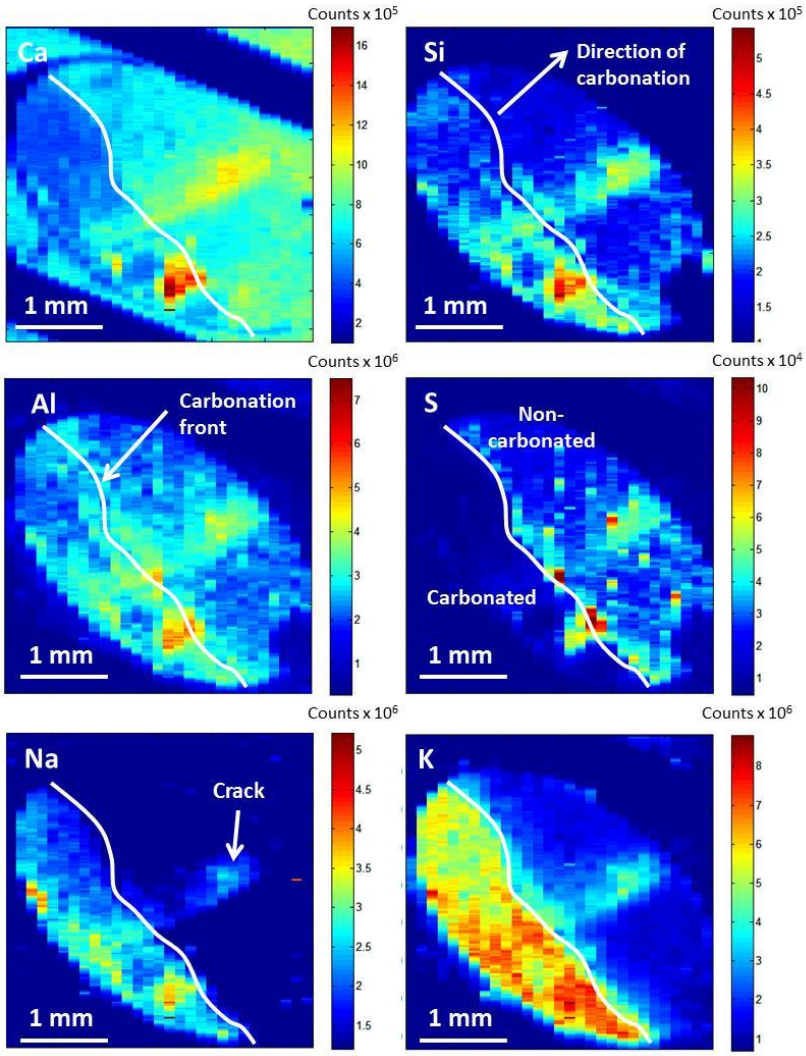

Figure 4. LA-ICP-MS maps showing the relative concentrations ~~The figure shows the elemental distributions~~ of Ca, Si, Al, S, Na and K in a partially carbonated sample of NRVB, corresponding to the region analysed by X-ray microtomography ~~(see Section 3.4. The presence of a carbonation front and transition zone is evident, separating areas of carbonated and non-carbonated NRVB~~.

~~The distributions of Ca, Si, Al and S in Figure 4 appear to be broadly consistent with those observed in Figure 3, giving further evidence for the decalcification of C-S-H in carbonated regions, but not yet full carbonation of an Al-rich ettringite or AFm phase ahead of the carbonation front. The acid digestion concentrations of Na and K were significantly different in the carbonated, partially carbonated and non-carbonated samples (Figure 2), indicating an enrichment of the alkali elements in the carbonated region. This is consistent with the elemental maps shown in Figure 4, where both Na and K are enriched in the carbonated region and depleted in the non-carbonated region. Furthermore, the distribution of both Na and K was lower in the vicinity of the front. The implications of these observations will be explored in more detail in Section 4.~~

3.4 X-ray microtomography

Selected slices of the representative volume of interest (VOI, 601×601×601 voxels at 5 μm resolution) for samples assessed from Cores 6.1 and 9 are shown in Figure 5. The brightest isolated phase regions ~~are~~ were assigned to unreacted Portland cement particles [Galluci *et al.*, 2007]. In the case of the partially carbonated regions (Figure 5(b) and (e)) there ~~is~~ was also a very bright feature corresponding to the accumulation of carbonation reaction products ~~accumulating in~~at the carbonation front. This difference in brightness indicates that the density of the carbonation front is higher than that of the other material. Voids appeared as darker areas [Galluci *et al.*, 2007] and were clearly identified by their spherical morphology in all samples assessed.

Commented [LB44]: this relates to permeability. How can you have a more dense microstructure by micro-CT yet a more permeable material?

We should amend the text regarding micropermeability. There is not a statistical difference between the carbonated and non-carbonated regions.

Commented [EJB45]: Agree also worth discussion on whether a denser material and a higher permeability can be reconciled

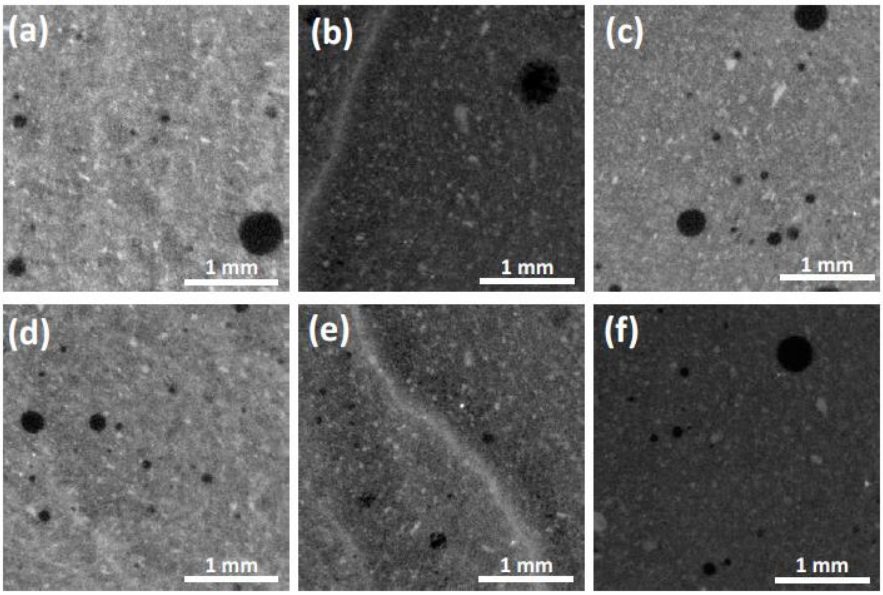

Figure 5. ~~The images show s~~Selected slices through the VOIs in each region of core~~ -~~: (a) and (d) ~~are for the~~ carbonated regions~~,~~: (b) and (e) ~~for the~~ partially carbonated regions~~,~~ and: (c) and (f) ~~for the~~ uncarbonated regions, ~~all~~ of Core 6.1 and 9 respectively.

~~For quantification of the results, segmentation of the VOI was carried out, thresholded based on identification of local minima in the greyscale histograms [Landis and Keane, 2010].~~ 2D images of selected slices, and 3D reconstructions of the VOI, o~~f~~ ~~the sample from~~ Core 9 are shown in Figures 6 and 7, respectively. The carbonated region (Fig~~ure~~ 6 ~~(~~a~~)~~) ~~has~~ had a reduced fraction of pores compared ~~with~~ to the uncarbonated region (Fig~~ure~~ 6 ~~(~~c~~)~~) due to the formation of calcium carbonate in the pore space. In the partially carbonated sample (Fig~~ure~~ 6 ~~(~~b~~)~~), at least two carbonation fronts ~~are~~ were identified in the VOI selected. Although the~~y carbonation fronts~~ are quite distinct, the formation of more than one front indicates that carbonation is neither occurring homogeneously throughout the sample, nor as a ~~simple,~~ single-step process at one sharply defined carbonation front~~. . This is consistent with the microstructural changes occurring during hydration, and the gradients in CO_2 concentration and humidity induced by the introduction of the CO_2 gas from an~~.

Commented [C46]: This is in the methodology, so no need to repeat here.

~~enclosed reservoir here. A~~The ~~higher~~ highest porosity was observed in the transition zone just behind the carbonation front ~~than anywhere else in the samples~~.

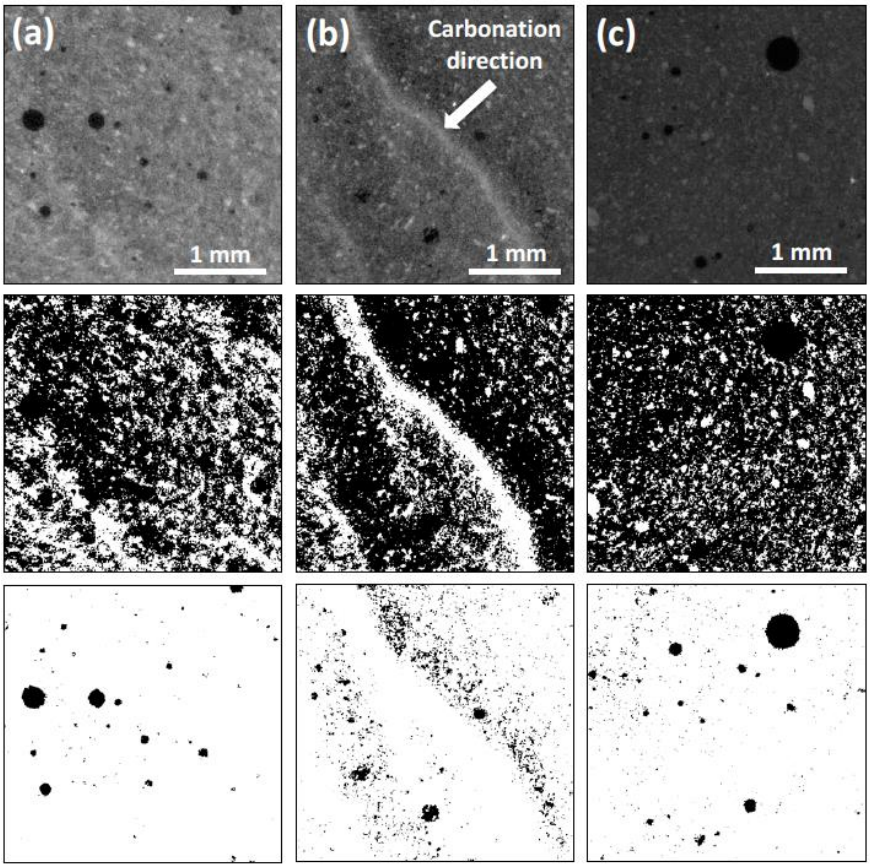

Figure 6. ~~The images show~~ 2D VOI reconstructions of samples from Core 9. The top row shows grey scale images, the centre row the images segmented into solid (white) and pore (black) regions, and the bottom row the images segmented into areas of large pores (black) of: ~~.~~ ~~The~~ (a) ~~column represents~~ the carbonated region; ~~the~~ (b) ~~column~~ the partially carbonated region, and; ~~the~~ (c) ~~columns~~ the uncarbonated region.

Formatted: Left

The 3D reconstructions of the VOI (Fig~~ure~~ 7) ~~are consistent with the observations of 2D results shown in Figure 6. The images in Figure 6 are individual slices (horizontal orientation) through the samples, whereas the images in Figure 7 are side-on views of the reconstructed stack of slices. The slices in Figure 6 would thus be viewable if looking down from the top of the 3-dimensional stacks as shown in Figure 7. It is clearly seen that there~~indicate a ~~is a~~ higher fraction of large pores were present in the uncarbonated region (Fig~~ure~~ 7 ~~(~~c)~~) than in the carbonated region (Figure 7 (a)),~~ and that there ~~is~~ was a high fraction of pores in the vicinity of the carbonation front, particularly just ahead of the very dense (bright) region in the sample (Fig. 7b).

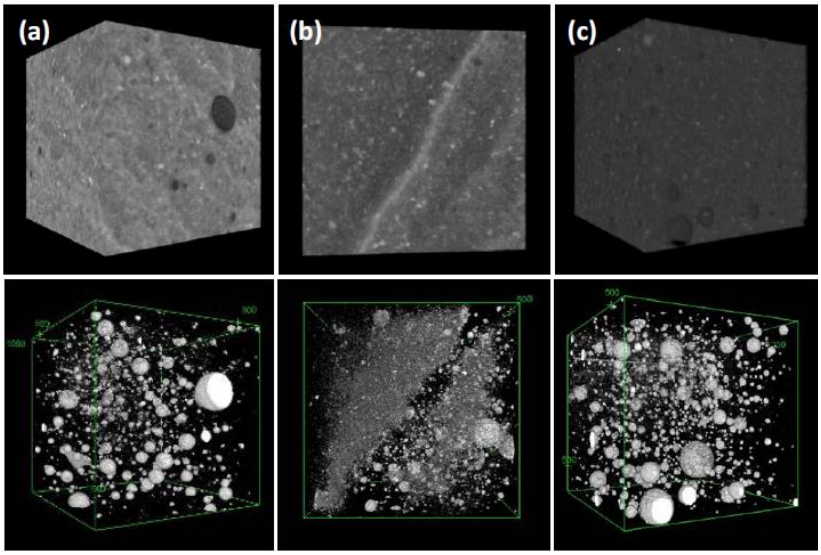

Figure 7. ~~The images show~~ 3D reconstructions of the VOI (top row) and the VOI re-thresholded to show only the large pores (bottom row), of the sample from Core 9~~.~~: ~~The~~ (a) ~~column represents the~~ carbonated region~~,~~; ~~the~~ (b) ~~column the~~ partially carbonated region (carbonation is from top left ~~as shown~~corner)~~,~~ and; ~~the~~ (c) ~~column~~ the uncarbonated region.

The porosity determined from XCT analysis ~~of this data for two samples from Cores 6.1 and 9~~ is summarised in Table 3. The average segmented porosity of the carbonated region wa~~s~~ found to be ~30% lower than ~~that~~ in the uncarbonated region, ~~which~~ confirm~~s~~ing the hypothesis that carbonation products ~~are~~ precipitat~~inged~~ in pore space, resulting in an increase in density.

Commented [LB47]: it was these two samples which showed lower permeabilities earlier in the manuscript.

Table 3. Summary of segmented porosity results

Core		Regions		
		Carbonated	Partially carbonated	Uncarbonated
6.1				
	Sample 1	33.3	-	-
	Sample 2	22.0	41.4	37.9
9				
	Sample 1	36.5	-	-
	Sample 2	31.7	43.2	43.5
Average		30.9	42.2	40.7
SD[1]		6.2	1.2	3.9

Notes: [1] – Standard deviation.

3.5 Raman spectroscopy

Despite leaving the samples to photobleach, all ~~the spectra~~data recorded were detrimentally affected ~~still plagued~~ by fluorescence, ~~swamping almost the entire Raman signal and~~ leaving just the most intense bands visible. ~~Ordinary~~ Portland cements are known to fluoresce [Richardson *et al.*, 2010], and so while not entirely unexpected, the fluorescence was more severe than had been anticipated.

All of the spectra obtained showed the characteristic ν_1 carbonate band at 1085 cm^{-1}, attributed to either calcite or aragonite [Black, 2009]. No ~~There was never any~~

evidence of any other calcium carbonate polymorphs, or of carboaluminate phases was observed. In some of the more well-defined spectra it was possible to see a lattice vibration band at 280 cm^{-1} or the ν_4 carbonate band at about 710 cm^{-1}; these bands are attributed ~~to~~ to calcite~~calcium carbonate~~. There was typically an increase in the intensity of the carbonate bands within the carbonated zone compared to regions beyond the carbonation front, indicating higher concentrations of carbonate within the carbonated zone. Similarly, in isolated spectra away from the carbonation front it was possible to discern a weak band at ~360 cm^{-1} attributed to portlandite. It was not possible to identify any other species within the spectra. Indeed, the region 900 – 1030 cm^{-1}, where characteristic sulfate ν_1 bands are expected~~would be present~~, was examined closely, but no peaks were observed. This should not be taken as there having been no sulfate species present, but rather that fluorescence obscured any bands.

3.6 Mineralogical and elemental analysis

Commented [C48]: This section should probably go after the LA-ICP-MS since it is a refinement of that technique. No?

The distribution of major and minor elements was mapped using BSEM-EDXA for several regions of Core 6.1 closely matching those examined by other techniques.~~using micro-tomography.~~ Data acquired ~~The results for all other cores were very similar to these.~~

~~The BSEM-EDXA observations~~ across the principal carbonation front are presented in Figure 8, where~~and show that there is~~ a major change in the microstructure of the hardened grout upon carbonation can be observed. The~~is involves the~~ decomposition of the fine-grained C-S-H gel matrix and the formation of a very fine-grained ~~inter~~mixture of calcium carbonate and silica-rich material at a micron scale can be observed, accompanied by the ~~formation~~ development of very concentric fine shrinkage cracks cemented by secondary calcium carbonate. This in agreement with ~~has been observed and described previously from and observed in~~ other experiments on the carbonation of NRVB and other Portland cements~~OPC based cements~~ [*e.g.* Rochelle and Milodowski, 2013].

Formatted: Highlight

Formatted: Font: Italic

In agreement with LA-ICP-MS results, ~~Carbonation also results in significant chemical changes and movement of major chemical components. T~~the EDXA elemental maps recorded across the main carbonation reaction front show that carbonation resulted in significant chemical changes and movement of major chemical components. In particular, ~~ are consistent with the LA-ICP-MS results, showing that~~ K and, to a lesser extent, Na were~~a~~ concentrated within the altered cement matrix behind the main carbonation front. Ca ~~has~~ was~~been~~ strongly concentrated at the reaction front and~~.~~ S ~~is~~ was depleted from the carbonated region behind the main reaction front, but ~~and is~~ enriched in the relatively unaltered region. ~~EDXA mapping shows that~~ Sulfur was ~~is~~ particularly concentrated immediately ahead of the main carbonation front where the calcium carbonate precipitation ~~is~~ was found to be dominant. In the uncarbonated region ahead of the reaction front, localized high concentrations of S, Al and Ca were observed in some samples~~, , which may facilitate the formation of ettringite or other calcium aluminosulphates, but this can ould only be confirmed by XRD. Theise wasere~~ particularly ~~observed~~ in large ~~pores~~ voids created by ~~due to the presence of~~ air-bubbles entrained within the grout during mixing, which would allow the expansive formation of ettringite. Chlorine ~~I is~~was present in the epoxy-resin used during sample preparation, so the map for Cl is a proxy for the resin-impregnated micro-porosity within the grout. The elemental maps across the reaction front show that Cl wa~~i~~s markedly depleted within the carbonated front compared to the remaining microstructure, suggesting a lower porosity and higher density in this region. This reduction in porosity is likely to result from the precipitation of calcium carbonate within the main porosity of the reaction front.

Commented [LB49]: this needs a ref. It also correlates with micro-CT but contradicts the current text regarding permeability

Formatted: Font color: Text 1

Commented [NC50]: ew Figure 8 from Tony.

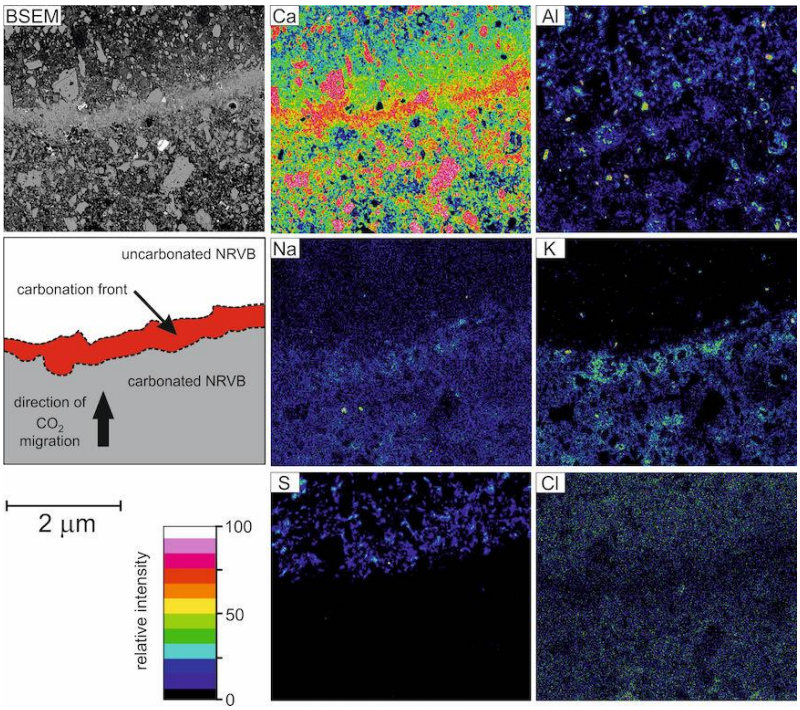

660

661 **Figure 8.** ~~The image shows a~~ BSEM image with corresponding colour-contoured
662 relative-intensity EDXA element distribution maps, recorded from a polished thin
663 section prepared across the carbonation reaction front for Core 6.1.

664

665 Areas far in front of the reaction front were also mapped, and showed that the cement
666 paste had not undergone intense alteration when compared to the grout within, and
667 behind, the main alteration front. In these regions C-S-H, calcium aluminate hydrates,
668 and partially hydrated cement clinker particles were still present. ~~There~~ However~~.~~,
669 ~~may have been~~ some carbonation of the portlandite and C-S-H gel in these regions
670 hased clearly occurred (Figure 9). Although "primary" calcium carbonate is present in
671 the NRVB as limestone flour added during the preparation of the NRVB cement,
672 these limestone particles are readily distinguished petrographically from the
673 secondary calcium carbonate produced by cement carbonation. The limestone flour
674 particles are characterized by angular fragments of calcium carbonate disseminated
675 throughout the NRVB samples (Figure 9). In contrast, secondary calcium carbonate
676 formed by carbonation reaction is manifested as fine-grained secondary calcium

carbonate forming alteration fringes around the margins of portlandite crystals or in irregular patches replacing C-S-H matrix material (Figure 9). Secondary calcium carbonate was also sometimes observed nucleating around limestone flour fragments. EDXA analyses and X-ray maps show that the secondary calcium carbonate forms fringes around portlandite crystals (Figure 9). Semi-quantitative compositional estimates from EDXA show the secondary carbonate fringes have a Ca:O ionic ratio (~0.3) similar to that of the limestone fragments (Ca:O ~0.34), implying that the carbonation reaction product is essentially $CaCO_3$ (Ca:O = 0.33). In contrast, the relatively unaltered cores of the partially-carbonated portlandite crystals have a much higher Ca:O ionic ratios that vary between calcium carbonate (0.33) and portlandite (0.5). The armouring of the surface of these portlandite crystals by a reaction rim of secondary calcium carbonate will probably have protected or limited reaction with CO_2 to some extent. ~~to produce very fine grained calcium carbonate , but this was difficult to confirm by BSEM.~~

~~This phenomenon was best observed around the margins of primary limestone grains, where secondary calcium carbonate may be nucleating as has been reported elsewhere [Milodowski *et al.*, 2013].~~

Commented [LB51]: especially given that the NRVB contained calcite as a starting material.

Commented [AM52R51]: This is now answered by the inclusion of a new figure – Figure 9 – which clearly illustrates the carbonation of portlandite in the cement matrix ahead of he main carbonation front.

The petrographic text is now expanded to give more detail of the carbonation fabrics observed *ahead* of the main carbonation front

Commented [LB53R51]: I think that this is fine. We know phenolphthalein is not a 100% accurate indicator of the position of a carbonation front.

Commented [LB54]: we need an image of these.

Commented [AM55R54]: This is now answered by the inclusion of a new figure – Figure 9 – which clearly illustrates the carbonation of portlandite in the cement matrix ahead of he main carbonation front.

The petrographic text is now expanded to give more detail of the carbonation fabrics observed *ahead* of the main carbonation front

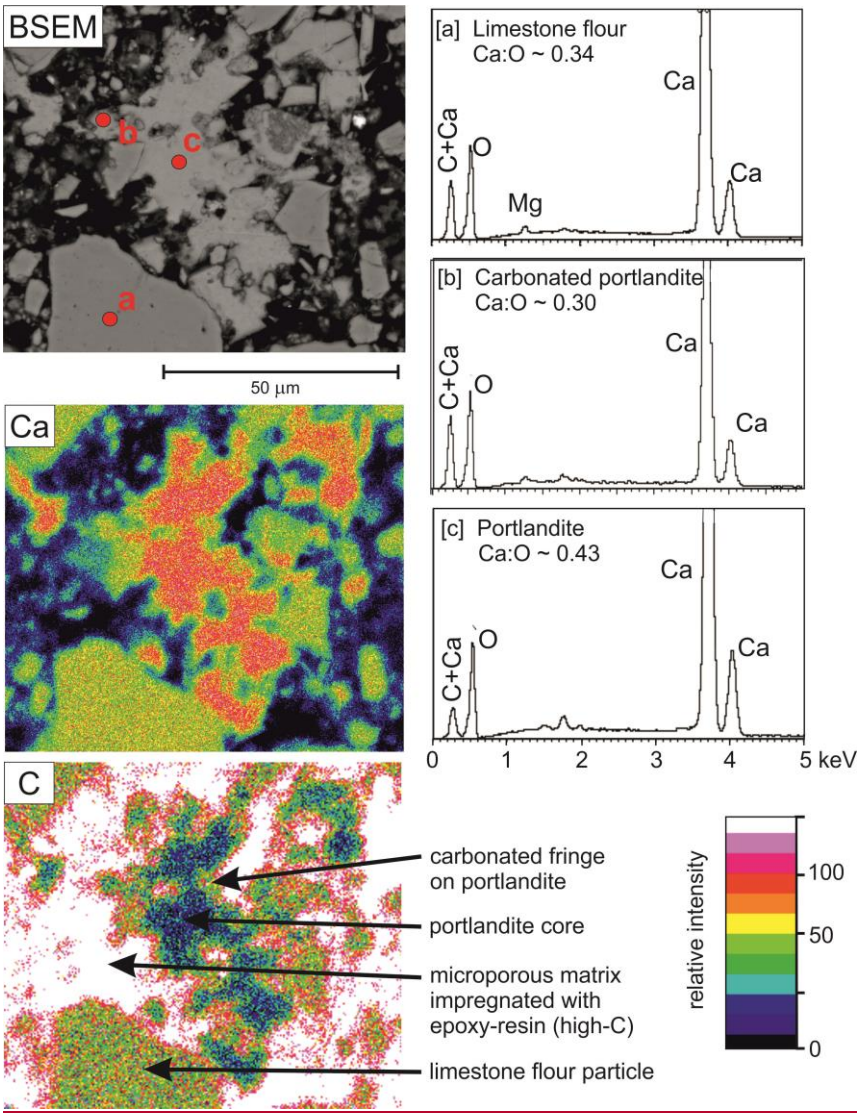

694

695 **Figure 9.** BSEM image with corresponding colour-contoured relative-intensity
696 EDXA element distribution maps for Ca and C, showing angular fragments of
697 limestone flour, and the development of a calcium carbonate alteration fringe around
698 a patch of poikiloblastic portlandite nucleated within the hydrated cement matrix.
699 Example EDXA spectra are also illustrated for: (a) a primary limestone flour particle;
700 (b) the carbonated reaction fringe around poikiloblastic portlandite, and; (c) the
701 relatively unaltered core of the portlandite. Recorded from a polished thin section

prepared 100 mm from the vent inlet, and 90 mm ahead of the carbonation front, for Core 6.1.

3.7 XRD analysis

The concentrations of crystalline phases in ~~for the~~each of the ~~three~~ cores, and each of the carbonation zones was determined ~~, and the results are shown in~~ (Table 4)~~.~~ ~~together with the geometric relationship of analysed material to the carbonation zone and main carbonation front defined by petrographic analysis.~~

The main crystalline phase present in all samples was calcite (a polymorph of $CaCO_3$) with smaller amounts of aragonite (another polymorph of $CaCO_3$), dolomite ($CaMg(CO_3)_2$), portlandite ($Ca(OH)_2$), gypsum ($CaSO_4.2H_2O$) and quartz (SiO_2) also detected. The very small amounts of quartz and dolomite are unlikely to have formed during cement hydration and carbonation, and most probably represent impurities in the limestone additive used in the NRVB. Petrographic observations confirmed the presence of fine fragments of crushed quartz and dolomite. ~~Other more m~~Minor reflections were also tentatively identified for ~~ardealite (~~$~~Ca_2SO_4HPO_4.4H_2O$~~, where the main reflection is at a *d*-spacing of 7.78Å),~~ ettringite ($Ca_6Al_2(SO_4)_3(OH)_{12}.26H_2O$, where the main reflection is at ~9.6Å) and a broad reflection with a *d*-spacing of 7.78Å that may indicate the presence of calcium monocarboaluminate ($Ca_4Al_2(CO_3)(OH)_{12}.5H_2O$, which has a characteristic diffraction peak at around 7.6Å (cf. Lothenbach et al., 2008)). The calcium monocarboaluminate appears to be present throughout the cores and may represent a reaction product formed with the limestone flour, which would be consistent with other studies that have previously shown that calcium mono-~~carboaluminate~~ and ~~calcium~~ hemicarboaluminate ($Ca_4Al_2(CO_3)_{0.5}(OH)_{13}.5.5H_2O$) phases form in hydrated blended cements containing limestone additives (Matschei et al., 2007; Lothenbach et al., 2008). Calcium hemicarboaluminate was not identified in present study on carbonated NRVB grout. However, its absence is not inconsistent with the observations of Lothenbach et al (*op. cit.*) who observed that both mono-~~carboaluminate~~ and hemicarboaluminate formed after 2 to 7 days, the monocarboaluminate content then increased with time, whilst hemicarbonate disappeared after 14 days.

Commented [C56]: Yep, see Vasconcelos et al. (2018)

Commented [AM57]: I agree with Leon's comment that this most probably represents calcium monocarboaluminate and NOT ardealite, as originally interpreted. I have revised and re-written this section (highlighted) to deal with this. The results are now consistent with those found in other studies of blended cements with added limestone. This hopefully, answers John's comment (cf. Nick's comment below) about the absence monocarboaluminate too.

As discussed by Lothenbach det al. (2008), the lack of detection of Afm phases by XRD may be due to their poor crystallinity. This may go part-way to answering John's comment below.

Commented [NC58]: From John Provis. No AFm phases? Very surprised to not see any monocarbonate or hemicarbonate in there. See http://www.sciencedirect.com/science/article/pii/S0008884608000161 for discussion (Fig 7 showing expanded view of peak positions)

Other minor weak reflections at ~14 and ~7.1Å were also identified that may represent C-S-H phases (e.g. Biagioni et al., 2015). However, the identity of these phases could not be confirmed. No AFm phases were found in the post-experimental NRVB grouts. However, Lothenbach et al. (2008) also found the Afm phases to have very poor crystallinity, and with variable compositions, making them difficult to detect by XRD analysis.

~~possibly a chlorite mineral (an aluminosilicate clay mineral possibly containing Fe and/or Mg, where reflections at ~14 and ~7.1Å were identified). However, the presence of these minor phases could not be confirmed.~~

~~XRD analyses found no evidence for the presence of monocarbonate or hemicarbonate phases, which other authors have identified to form in hydrated blended cements cements containing limestone additives (Lothenbach et al., 2008). The absence of monocarbonate or hemicarbonate in the present study may be due to the way the NRVB grout was cured and maintained during the carbonation experiments. Lothenbach et al. (2008) undertook their XRD analyses on limestone blended cement pastes that were cured and maintained water saturated for up to 1 year. They observed that monocarbonate and hemicarbonate formed after 2 to 7 days, monocarbonate then increased with time, whilst hemicarbonate disappeared after 14 days. In contrast, the NRVB grout was not cured under water and maintained in a water saturated state during the carbonation experiments. This may have prevented the formation of monocarbonate or hemicarbonate in the present study. Afm phases were also not found in the post-experimental NRVB grouts. Lothenbach et al. (2008) also found these phases to have low crystallinity, with variable compositions making it difficult to detect them in XRD patterns. The non-detection of Afm phases in the present study may also be due to these phases being poorly crystalline or amorphous.~~

~~**Table 4. Summary of XRD results**~~

~~Core~~	~~Dist. From~~	~~Mineralogy (wt.%)[1]~~

Formatted: English (United States), Highlight

Commented [NC59]: Need to add ref.

Commented [NC60]: Added by Tony.

Commented [AM61R60]: Nick – please delete this text I provided previously, as I have revised and re-written the text above (see highlighted section)

	inlet										
		Calcite	Aragonite	Dolomite	Portlandite	Ettringite	Arcelite	Gypsum	Quartz	Kaolin	Chlorite
6.1	0.1	91.5	–	0.7	–	1.8	3.2	–	0.6	2.2	–
	0.7	91.2	–	0.6	–	1.7	3.3	–	0.9	2.3	–
	0.9	91.6	–	<0.5	–	1.7	3.2	–	0.9	4.0	–
	30.7	77.3	8.8	–	3.6	–	5.2	–	1.1	4.0	–
	48.8	75.5	8.0	–	4.7	–	5.7	–	1.9	4.2	–
9	0.2	91.8	–	0.6	–	–	2.8	2.4	<0.5	2.0	–
	0.6	90.8	–	0.6	–	–	3.2	2.2	0.9	2.3	–
	1.2	82.3	3.1	<0.5	1.8	2.6	3.3	3.1	1.0	2.6	–
	20.0	73.2	9.0	–	5.0	3.2	4.7	–	0.9	4.0	–
	44.8	74.4	7.6	–	5.3	3.1	4.7	–	1.1	3.8	–
12	0.1	93.6	–	0.6	–	–	3.6	–	<0.5	–	1.9
	0.5	90.7	–	0.6	<0.5	2.3	3.4	–	0.9	–	1.8
	0.7	60.2	–	–	24.0	7.7	5.0	–	0.8	–	2.3
	21.5	61.9	–	–	22.5	4.0	4.9	3.9	<0.5	–	2.4
	41.5	60.0	–	–	23.4	4.1	5.3	4.1	0.7	–	2.3

Notes: [1] wt.% of all crystalline material present.

Table 4. Summary of quantitative XRD results for crystalline components (normalised to 100%)

Core	Vertical distance from inlet vent(cm)	Relative mineral proportions (wt % normalised to 100%)[1]							Other minor phases[2]	Portlandite : total $CaCO_3$ (calcite +aragonite) ratio	Relationship to petrographically defined carbonation reaction front
		Calcite	Aragonite	Dolomite	Portlandite	Ettringite	Gypsum	Quartz			
6.1	0.1	96.7		0.7		1.9		0.6	Mono. 7.1 Å	0.000	Carbonated zone
	0.7	96.6		0.6		1.8		1.0	Mono. 7.1 Å	0.000	Carbonated
	0.9	97.2				1.8		1.0	Mono. 7.1 Å	0.000	Main carbonation reaction font

Commented [AM63R62]: Quartz and dolomite now discussed above – most probably impurities in the limestone additive.

Commented [AM63R62]: Quartz and dolomite now discussed above – most probably impurities in the limestone additive.

Commented [LB62]: Where do these come from? Quartz might be present in the original NRVB (I doubt it) but I cannot see where kaolin would come from.

Also, it is unfortunate that the analysis was not necessarily conducted before, at and after the carbonation front. We cannot see whether there is enrichment of ettringite just ahead of the carbonation front, but looking at the carbonation depths in table 2, I don't think that there is a correlation between the phenolphthalein depth and the XRD data. What we can say is that ettringite is decomposed by the aggressive carbonation regime (in line with the findings of Grounds et al.
T Grounds H G Midgley D V Novell Carbonation of ettringite by atmospheric carbon dioxide, Thermochimica Acta, 1988, 135, 347-352)

Commented [LB62]: Where do these come from? Quartz might be present in the original NRVB (I doubt it) but I cannot see where kaolin would come from.

Also, it is unfortunate that the analysis was not necessarily conducted before, at and after the carbonation front. We cannot see whether there is enrichment of ettringite just ahead of the carbonation front, but looking at the carbonation depths in table 2, I don't think that there is a correlation between the phenolphthalein depth and the XRD data. What we can say is that ettringite is decomposed by the aggressive carbonation regime (in line with the findings of Grounds et al.
T Grounds H G Midgley D V Novell Carbonation of ettringite by atmospheric carbon dioxide, Thermochimica Acta, 1988, 135, 347-352)

Formatted Table

Formatted Table

	30.7	85.1	9.7		4.0			1.2	Mono. 7.1 Å	0.042	Relatively unaltered NRVB distant from reaction front
	48.8	83.8	8.9		5.2			2.1	Mono. 7.1 Å	0.056	Relatively unaltered NRVB distant from reaction front
9	0.2	91.8	-	0.6	-	-	2.4	<0.5	Mono. 7.1 Å	0.000	Carbonated zone
	0.6	90.8	-	0.6	-	-	2.2	0.9	Mono. 7.1 Å	0.000	Main carbonation reaction font
	1.2	82.3	3.1	<0.5	1.8	2.6	3.1	1	Mono. 7.1 Å	0.021	Matrix immediately in front of reaction front
	20.0	73.2	9	-	5	3.2	-	0.9	Mono. 7.1 Å	0.061	Relatively unaltered NRVB distant from reaction front
	44.8	74.4	7.6	-	5.3	3.1	-	1.1	Mono. 7.1 Å	0.065	Relatively unaltered NRVB distant from reaction front
12	0.1	93.6	-	0.6	-	-	-	<0.5	Mono. 14.1 Å	0.000	Carbonated zone
	0.5	90.7	-	0.6	<0.5	2.3	-	0.9	Mono. 14.1 Å	0.000	Main carbonation reaction font
	0.7	60.2	-	-	24	7.7	-	0.8	Mono. 14.1 Å	0.399	Relatively unaltered NRVB distant from reaction front
	21.5	61.9	-	-	22.5	4	3.9	<0.5	Mono. 14.1 Å	0.363	Relatively unaltered NRVB distant from reaction front
	41.5	60	-	-	23.4	4.1	4.1	0.7	Mono. 14.1 Å	0.390	Relatively unaltered NRVB distant from reaction front

Notes:

[1] Normalisation excludes quantification of minor calcium monocarboaluminate and unidentified 7.1 Å and ~14 Å phases.

[2] "Mono." = calcium monocarboaluminae; "7.1 Å" = unidentified phase; "14 Å" = unidentified phase.

Quantification of the absolute composition the NRVB samples by XRD is problematic. Petrographic observations indicate that there is a significant amount of C-S-H and AFm material present in the largely unaltered cement matrix ahead of the main carbonation front. These phases are disordered or amorphous, and are not easily detectedable by XRD. Therefore, the quantitative XRD data presented in Table 4 only represent the "relative" proportions of the crystalline phases present. This, together

with a large proportion of the calcite present representing original limestone flour additive, means that the extent of carbonation cannot be evaluated simply from the total relative amounts of calcite and aragonite alone. However, because carbonation involves the replacement of portlandite (as well as C-S-H) by calcium carbonate (as shown by petrographic analysis), the amount of portlandite relative to the total amount of calcium carbonate (calcite + aragonite) should provide an indicator of how deep carbonation has occurred in the grout.

The portlandite : total $CaCO_3$ ratios based on the XRD results is presented in Table 4. The detection of portlandite is a key marker of regions that are not yet fully carbonated, and appears to correlate with the radial distance of the sample from the centre of the vent. The XRD data show that portlandite has completely reacted to form calcium carbonates within the reaction front and the main carbonated zone behind this front. The relatively unaltered cement ahead of the- main reaction front still contains significant portlandite. However, the portlandite : total $CaCO_3$ ratios progressively increase with increasing distance from this front. This implies that carbonation has occurred in the cement ahead of the main reaction front (where complete carbonation has occurred) but that this diminishes with increasing distance. This is consistent with the BSEM-EDXA petrographic observations, which showed patchily-distributed secondary fine-grained calcium carbonate replacing and armouring portlandite and C-S-H in the cement matrix ahead of the main reaction front (see previous discussion in Section 3.6 and illustrated in Figure 9.

Core 12 appeareds to be anomalous, compared to cores 6.1 and 9, with respect to the portlandite content of the relatively unaltered grout. The amount of portlandite preserved in this core appearss to be significantly higher than the other two cores, and may reflect some degree of heterogeneity of carbonation within the experimental waste drum.

Aragonite was identified within the uncarbonated material ahead of the main reaction front, but is absent in the main carbonated grout regions. Significant aragonite is metastable and unlikely to have been present in the original limestone flour additive. Therefore, the aragonite is likely to be a reaction product in the cement, and may provide some further indication of depth of penetration and reaction of CO_2 ahead of

the main carbonation front. It would appear that if aragonite had -formed initially within the main carbonated zone, it has subsequently been replaced by calcite as the degree of carbonation alteration progressed.

~~The regions of carbonated grout behind the main reaction front contained high quantities of calcite (typically >80%). The areas closest to the centre of the vent and base of the vessel contained the highest calcite content, whereas the least amount was detected in the areas at the edge of vessel and furthest from the vent. Regions located between the two contained an intermediate quantity of calcite.~~

~~In most cases portlandite or aragonite were not detected in the carbonated regions, but small amounts were found distant from the centre of the vent (200mm and at the vessel edge). The detection of portlandite, which is a key marker of regions that are not yet fully carbonated, appears to correlate with the radial distance of the sample from the centre of the vent; portlandite was detected in the main alteration zone only in the samples furthest from the centre of the vent.~~

~~The uncarbonated zones ahead of the alteration front also contained significant quantities of calcite as the NRVB contains added limestone flour, but the amounts were typically lower (55-75%) than in the corresponding carbonated zones. The uncarbonated regions also typically contained higher quantities of portlandite than in the carbonated regions.~~

~~Aragonite was identified in some samples within the uncarbonated material ahead of the main reaction front, but there was no identifiable trend between aragonite concentration and location of the samples from the vent. A significant amount of the calcite determined by XRD can be attributed to limestone flour that was originally added in the NVRB formulation (Table 1). However, the amount of calcite present in the 'nominally uncarbonated zone' identified by phenolphthalein staining is too great (over 80 wt.% in some subsamples: Table 4, Figure 8) to be due to the limestone flour additive alone. This indicates that significant carbonation of the NRVB cement matrix has proceeded ahead of the visible carbonation front. This was confirmed by BSEM-EDXA petrographic observations, which showed fine-grained calcium carbonate replacing the cement matrix in diffuse, irregular patches.~~

Commented [NC64]: Added by Tony.

In terms of the minor mineral phases, quartz and dolomite are phases within the limestone flour used in the grout. Gypsum, ettringite and calcium monocarboaluminate ~~and ardealite~~ are likely to be secondary precipitates formed during the hydration of the cement in the grout. These minor phases could not generally be discriminated during petrographic analysis (BSEM-EDXA) because of their low concentration, their fine grain size and the intimate mixing of the hydrated cement phases. However, discrete coarse crystals of ettringite were observed in large voids ~~pore space~~ in the hardened grout that represent air bubbles that were originally entrained in the cement paste during mixing, and that were previously occupied by air or water. There was no obvious relationship between the distributions of these minor phases and the carbonation front. ~~Ardealite was tentatively identified as a very minor component on the basis of very weak X-ray reflections but no evidence for it was found during petrographic analysis.~~

4. ~~Further~~ Discussion

Using LA-ICP-MS, micro-tomography and EDXA three distinct regions were identified in each sample, 1) carbonated, 2) partially carbonated and 3) uncarbonated. A carbonation front and a transition zone were identified in the partially carbonated region. Analysis by LA-ICP-MS and EDXA showed that K and Na ~~are~~ were concentrated within the carbonated regions behind the main reaction front, and the concentration wa~~i~~s greatest in a narrow zone up to 1-2mm wide immediately at the rear of where the Ca ~~is~~ was concentrated within the main reaction front. The carbonation front ~~is~~ was enriched in S and Al, and the former ~~is~~ was depleted from the carbonated region at, and behind, the main reaction front. Micro-tomography results indicated that the porosity of the carbonated region wa~~i~~s lower than in the uncarbonated region due to deposition of secondary calcium carbonate within the pore space of the hardened grout (as confirmed by BSEM/EDX); however, micro-permeametry results showed that the grout ~~is~~ was more permeable in the carbonated region. This higher permeability may be due to greater interconnectivity of micro-fractures within the pore network.

Similar porosity results to those obtained here have been reported by Hills *et al.*

Formatted: Highlight

Commented [NC65]: From John Provis. I've never before seen this as a cement hydration product, how convinced are we of its existence/presence here?

Commented [AM66]: Delete this in the light of the revisions above

Commented [C67]: This a pure repetition of what is written in the results. It's fine, but the results need a complete re-write to avoid the repetition. I'm not criticizing, because I know it's difficult to put the words of several authors together, but in this state, the paper won't be accepted by a (good) journal, which I think RWM would prefer.

Commented [LB68]: This supports the suggestion that the label in the first column of table 2 should be "mm" not "cm".

Commented [C69]: Wrong word – choose another!

Commented [LB70]: I don't agree. There are 2 data points for core 6 and 1 for core 9 which are clearly outliers. Excluding these and there is no difference between the carbonated and non-carbonated regions.

Commented [C71]: Or the detection limit of the technique?

Commented [EJB72]: Agree that we need a discussion on this - Ed

885 [1999], who used SEM to identify a porosity reduction of up to 26% in hardened
886 cemented wasteforms subjected to accelerated carbonation. Lange *et al.* [1996] have
887 also reported increased mechanical strength in carbonated cement wasteforms, which
888 they associated with the precipitation of calcium carbonate products in the specimen
889 pores, and an increase in density and reduction of the total porosity. The porosity of
890 the partially carbonated region is similar to that of the uncarbonated region, and
891 Figures 6 and 7 show that there is an increase in porosity near to the carbonation
892 front.
893
894 The higher permeability of the carbonated regions when investigated by micro-
895 permeametry appears at first to contradict the petrographic observations and the X-
896 ray micro-tomography results, which indicate that the porosity of the carbonated zone
897 is reduced in comparison to the unaltered cement. However, this may be because the
898 micro-porosity in the carbonated cement is more interconnected than in the unaltered
899 cement matrix. The petrographic analysis showed the presence of micro-fractures in
900 the carbonated region (described as fine shrinkage cracks), and whilst these micro-
901 fractures largely appeared to be cemented by secondary calcium carbonate reaction
902 product, the presence of some uncemented micro-fractures may provide a network of
903 higher permeability pathways within the altered cement.
904
905 The LA-ICP-MS results suggest that alkali ions are released from the cement
906 component of the NRVB grout during the hydration of the ~~O~~PC powder, and become
907 distributed between the aqueous solution and the precipitating C-S-H phases
908 [Lothenbach *et al.*, 2008]. The results shown here suggest that the carbonation of C-S-
909 H phases corresponds to enhanced alkali concentrations, evidenced by the higher
910 concentration of Na and K in the carbonated regions of the samples. In their study of
911 the carbonation of ~~O~~PC pastes, Anstice *et al.* [2005] reported a decrease in Na and K
912 concentration in the pore solution extracted from carbonated samples *cf.* uncarbonated
913 material, which is the opposite of the results presented here. They postulated that this
914 was due to enhanced binding of alkali metals to the solid products of carbonation,
915 which they stated was most likely to be by the hydrous silica gel formed during
916 decalcification of C-S-H. Because the concentrations of Na and K were lower in the
917 immediate vicinity of the carbonation front in our work, it may be hypothesised that
918 either 1) C-S-H carbonation is not the main process that occurs in the vicinity of the

Commented [LB73]: I don't think this is needed if we accept that there are outliers in the permeability data.

Commented [EJB74]: As above need a phone discussion on this. Ed

Commented [EJB75]: I'd agree with Leon's LB56 point below. Wouldn't we expect the carbonates of K and Na to be less soluble than the hydroxides?

carbonation front (which would be consistent with the fact that the large additional quantity of $Ca(OH)_2$ contributed to the NRVB by the slaked lime component of its formulation must also carbonate, compared to the much lower content formed in Portland cement hydration), or 2) that C-S-H carbonation is slower in this region; these may be the reasons why the interfacial region at the carbonation front in our work has a higher porosity than the fully-carbonated region.

The results from the X-ray micro-tomography studies warrant further discussion. In a recent study, Morandeau *et al.* [2014] evaluated the carbonation of pure Portland cement binders *via* a gamma ray attenuation method (GRAM), and also identified a reduction in the total porosity of carbonated specimens; however, they observed densification in the vicinity of the surface where carbonation seemeds to be stabilised, which differs from the results observed in this study. The discrepancy between that study and the NRVB results reported here could be associated with differences in the chemistry of NRVB and hydrated plain Portland cement as noted above, leading to differences in the kinetics of carbonation of the reaction products forming in these binders, or the differences in resolution of GRAM *vs.* micro-tomography, so that the increase in the porosity near the carbonation front could not be detected by GRAM. It has been proposed [Villain *et al.*, 2007] that under natural carbonation conditions, the carbonation of portlandite and C-S-H occurs simultaneously, even though from a thermodynamic perspective carbonation of portlandite prevails over CSH carbonation [Glasser and Matschei, 2007]. Morandeau *et al.* [2014] have observed that the initial rates of carbonation of these phases are comparable, but while carbonation of C-S-H continues to take place, the carbonation of portlandite reduces and stops during the time of CO_2 exposure.

Additionally, it was proposed [Morandeau *et al.*, 2014] that the carbonation of C-S-H is the main contributor to pore clogging, with the effects depending on its Ca/Si ratio, while dissolution of portlandite via carbonation can increase the porosity to partially counteract the pore-blocking effects of $CaCO_3$ precipitation. Considering this, it is likely that dissolution of calcium hydroxide, along with carbonation of ettringite and AFm phases, with a limited extent of decalcification of the C-S-H phases, could be taking place in the vicinity of the carbonation front, thereby reducing the precipitation of carbonation product in the pores of this region. This hypothesis is consistent with

Commented [LB76]: I'm not sure about this. Anstice et al analysed the pore solution, we've analysed the solid. Therefore, you would expect the two to be different.

It is also important to note that we have a higher portlandite content and less C-S-H than in OPC. However, the use of pure CO2 will also have an effect, where C-S-H is more likely to be carbonated than at atmospheric levels (Castellote et al).

Formatted: Font: Italic

Commented [LB77]: Again, this seems to stem from the outlying permeability measurements.

Commented [LB78]: Morandeau showed that C-S-H shrinks upon carbonation, but CH carbonation leads to an increase in volume. In normal cements the two almost cancel out and there is a slight reduction in porosity. In our case, there is far more CH so the overall effect would be a reduction in porosity.

Commented [LB79]: the situation in pure CO2 is different, with simultaneous carbonation of CH and C-S-H. In part this is due to steric effects with CH crystals covered with carbonation products, so preventing their further carbonation.

Commented [LB80]: My more recent results (from Julia Herterich, but as yet unpublished) showed carbonation of portlandite to occur prior to carbonation of the C-S-H. Only once the CH had carbonated did the C-S-H begin to carbonate significantly. i.e. the portlandite acts as a carbonation buffer.

Given the observation that carbonation of CH leads to a reduction in porosity, while carbonation of C-S-H leads to an increase, and that the NRVB has a much higher portlandite content, this would support a decrease in porosity upon carbonation of NRVB. This is in line with SEM and micro-CT, but not with permeability. Hence my concerns over permeability data (more specifically the last couple of data points for 2 of the 3 cores).

Commented [LB81]: I read Morandeau's paper very differently. Carbonation leads to decalcification of the C-S-H which leads to shrinkage. In turn calcium carbonate precipitation leads to pore blocking. There is only an increase in porosity if the CH dissolves and does not precipitate calcium carbonate. This is not the case in our work.

the LA-ICP-MS results, where a reduced concentration of alkalis in the vicinity of the carbonation front was observed, where higher concentrations of alkalis were associated with their potential binding to solid carbonation products and the hydrous silica gel forming during decalcification of C-S-H in this area.

The conditions used to induce carbonation also have a significant impact on how this phenomenon proceeds, and therefore it is important to consider that the NRVB evaluated in this study was carbonated under conditions of high CO_2 pressure, when compared to the 1-4kPa partial pressure used in most cement/concrete carbonation tests (with the exception of 100% CO_2 or supercritical conditions used in occasional specialised work). Under those conditions, the carbonation of the C-S-H phase is known to prevail over carbonation of calcium hydroxide as a consequence of the formation of crystalline calcium carbonate on the surface of the calcium hydroxide, inhibiting its further dissolution [Hidalgo *et al.*, 2008; García-González *et al.*, 2006]. Densification of samples carbonated under high CO_2 pressures has been identified, consistent with the theory of pore clogging due to carbonation of CSH as suggested by Morandeau *et al.* [2014]. This further supports the hypothesis that in the vicinity of the carbonation front of the NRVB evaluated, dissolution of portlandite via carbonation to produce calcium carbonate, along with limited decalcification of C-S-H, are the main degradation processes taking place in this region.

Commented [LB82]: there's a lot of studies using 100% CO2. What you have written next is important. When using 100% CO2 you get more C-S-H carbonation than under atmospheric conditions.

In analysing the XRD results further, it is relevant to discuss the following points in more detail. There is significant formation of secondary calcium carbonate behind the main reaction front (defined by the extent of phenolphthalein staining). Within the main carbonated region behind the reaction front, nearly all the portlandite, C-S-H and calcium (sulfo)aluminate hydrate phases are replaced by calcite. Calcite is the principal carbonate phase precipitated, although a small amount of aragonite is sometimes present.

T~~However, t~~his study also demonstrates that the impact of carbonation extends well beyond the apparent limit of reaction indicated by phenolphthalein staining, and reaction has occurred throughout the sample. Even in the regions furthest from the centre of the vent, where phenolphthalein staining ~~indicates~~ suggests that carbonation has not taken place, the XRD and petrographic observations ~~results indicate~~ show that

portlandite and C-S-H have partially-reacted with CO_2 to produce secondary calcium carbonates. This is reflected in the portlandite : $CaCO_3$ ratio, which progressively decreases with increasing distance from the reaction front, and by the presence of portlandite crystals armoured by reaction rims of $CaCO_3$ in the "relatively unaltered" cement. ~55 – 75 % of the crystalline phases present is calcite, and up to 9 % is aragonite. The total calcium carbonate content of the regions indicated by phenolphthalein staining to be uncarbonated is well in excess of the 28.61 wt.% of limestone flour in the original grout (or 44.39 wt.% of the total solids content), so theThe XRD and petrographic results clearly indicate that the extent of carbonation is underestimated by phenolphthalein staining. These observations are consistent with other studies which also found that significant carbonation of NRVB grout occurred ahead of the main visibly distinct carbonation reaction front [Rochelle and Milodowski, 2013]. The petrographic observations clearly showed the growth of secondary calcite within the partially carbonated grout matrix. Petrographically, it is possible to differentiate between the calcite originally present in the limestone flour and the secondary calcite formed from the carbonation of other phases, and this supports the observations made using XRD. Finally, there appears to be a distinct relationship between the amount of carbonation and the radial proximity to the centre of the vent; material closest to the vent has been carbonated more than material further away from the vent.

Needs a section here on "so what?" for geological disposal of nuclear waste?

5. Conclusions

Our investigations have shown that The main conclusions resulting from this work are:

- Ccarbonation of NRVB does not proceed as a horizontal carbonation front, but by a radial front with carbonation occurring well beyond the main reaction front.
- Three distinct regions were identified in the hardened NRVB grouts; carbonated, partially carbonated and uncarbonated. Within the partially carbonated region, a carbonation front and a transition zone were discerned.

Formatted: Subscript

Commented [NC83]: From John Provis.
I'm concerned about this conclusion being highlighted so strongly, as I'm not convinced it's correct. The uncarbonated region should contain a significant level of C-S-H, which is disordered and so excluded from the XRD quantification, and the AFm phases may also be quite disordered. If the hydrated NRVB was say 30% disordered phases (C-S-H + low-crystallinity AFms, which is quite feasible), that would match the XRD results to the original recipe very closely and not need the assumption of carbonation ahead of the front?

Commented [AM84R83]: I hope this is now answered to some xtent by the revised and motre complete describtion of XRD and petrographic fresults (together with images) given above.

Commented [NC85]: From John Provis.
I don't think this comparison is valid – the paper cited is on borehole cements, not NRVB, and the experimental work there was based on CO2-saturated brine rather than gas exposure?

Commented [AM86R85]: Agree – I have deleted this text comparing the results to previous carbonation studies by Rochelle and Milodowski, 2013)

Commented [NC87]: From John Provis.
Do we have the data to show this?

Commented [AM88R87]: We now describe and illustrate this in detail in the Petrography section, including new images

Commented [C89]: Too long, needs re-writing

Formatted: Normal, No bullets or numbering

- K and to a lesser extent Na ~~are~~ were concentrated within a 1-2 mm deep zone in the carbonated region just ahead of the main reaction front, and ~~.~~
- ~~T~~the area just ahead of the carbonation front ~~is~~ was enriched in both S and Al~~;~~ ~~and~~ S ~~is~~ was depleted from the carbonated material behind the main reaction front.
- Within the main carbonated region, virtually all of the hydrated cement phases (portlandite, calcium silicate hydrate and calcium aluminate hydrate) ~~are~~ were carbonated and calcite ~~is~~ was the predominant phase. Aragonite is also formed, but this appears to be initially formed ahead of the main reaction front, and is possibly destabilized, replaced and altered to calcite as more extensive carbonation proceeds.
- Some carbonation had occurred throughout the canister. Even within material indicated by phenolphthalein solution to be uncarbonated, partial carbonation had occurred.
- The porosity of the carbonated grout ~~is~~ was lower than in the uncarbonated material due to replacement of pore space with precipitated calcium carbonate. However, the highest porosity was observed in the partially carbonated region.

Commented [NC90]: From John Provis.
See comment on Page 30.

Commented [AM91R90]: Please no see revised text for XRD and petrography, which shows this is occurring

Commented [LB92]: you say the opposite to this on page 12

6. Acknowledgements

The authors acknowledge the contribution of S Williams at Radioactive Waste Management in funding the experimental work that led to the preparation of this paper. The X-ray microtomography work was conducted at the Manchester X-ray Imaging Facility, and the authors thank the technical staff of that facility for their assistance in scanning the samples and calculating reconstructions. We thank Neil Bramhall for assistance with LA-ICP-MS measurements. AEM, LPF, SJK, IM and AB publish with the permission of the Executive Director of the British Geological Survey (NERC). CLC is grateful to EPSRC for the award of an ECR Fellowship (EP/N017374/1). Portions of this work were performed at the MIDAS Facility, at the University of Sheffield, which was established with support from the Department of Energy and Climate Change.

References

Anstice, D. J., Page, C. L., Page, M. M., 2005. The pore solution phase of carbonated cement pastes. Cem. Concr. Res. 35, 377-383.

Atkins, M., Glasser, F.P., 1992. Application of Portland cement-based materials to radioactive waste immobilization. Waste Manage. 12, 105-131.

Biagioni, C., Merlino, S., Bonaccorsi, E. 2015. The tobermorite supergroup: a new nomenclature. Mineralogical Magazine, 79, 485-495.

Bary, B., Sellier, A., 2001. Coupled moisture—carbon dioxide–calcium transfer model for carbonation of concrete. Cem. Concr. Res. 34, 1859-1872.

Basheer, L., Kropp, J., Cleland, D.J., 2001. Assessment of the durability of concrete from its permeation properties: a review. Constr. Build. Mater. 15, 93-103.

Black, L., 2009. Raman spectroscopy of cementitious materials. In: J. Yarwood, R. Douthwaite, S. Duckett, (editors), Spectroscopic Properties of Inorganic and Organometallic Compounds, 40, Royal Society of Chemistry, UK, 72-127.

Black, L., ~~Gerbev~~Garbev, K., Gee, I., 2008. Surface carbonation of synthetic C-S-H samples: A comparison between fresh and aged C-S-H using X-ray photoelectron spectroscopy, Cem. Concr. Res. 38, 745-750.

BS 594-1:2005, Hot rolled asphalt for roads and other paved areas. Specification for constituent materials and asphalt mixtures, British Standards Institution, 2005.

BS EN 459-1:2015, Building lime. Definitions, specifications and conformity criteria, British Standards Institution, April 2015.

Cann, G. C., Orr, R. M., 2010. A technical specification for Portland cement, blast furnace slag and fly ash for use in the encapsulation/immobilisation of radioactive waste materials (8th Revision), NNL 10653.

Collier, N. C., 2016. Transition and decomposition temperatures of cement phases – a collection of thermal analysis data, Ceramics-Silikáty 60, 338-343.

Fernández-Bertos, M., Simons, S. J. R., Hills, C. D., Carey, P. J., 2004. A review of accelerated carbonation technology in the treatment of cement-based materials and sequestration of CO_2. J. Hazard. Mater. B112, 193-205.

Francis, A. J., Cather, R., Crossland, I. G., 1997. Development of the Nirex Reference Vault Backfill; Report on Current Status in 1994, S/97/014.

Gallucci, E., Scrivener, K., Groso, A., Stampanoni, M., Margaritondo, G., 2007. 3D experimental investigation of the microstructure of cement pastes using synchrotron X-ray microtomography (μCT). Cem. Concr. Res. 37, 360-368.

Garboczi, E. J., Bentz, D. P., 2001. The effect of statistical fluctuation, finite size error, and digital resolution on the phase percolation and transport properties of the NIST cement hydration model. Cem. Concr. Res. 31, 1501-1514.

García-González, C. A., Hidalgo, A., Andrade, C., Cruz Alonso, M., Fraile, J., López-Periago, A. M., Domingo, C., 2006. Modification of composition and microstructure of Portland cement pastes as a result of natural and supercritical carbonation procedures. Industrial Engineering Chemistry Res. 45, 4985-4992.

Glasser, F., Matschei. T., 2007. Interactions between Portland cement and carbon dioxide. in: Proceedings of the 12th International Congress on the Chemistry of Cement. Montreal, Canada.

Harris, A. W., Boult, K. A., Manning, M. C., Tearle, W. M., 2003a. Experimental study of carbon dioxide uptake by NRVB and 3:1 BFS/OPC, Serco Report Serco/ERRA-0453.

Harris, A. W., Manning, M., Tearle, W. M., 2003b. Carbonation of Nirex Reference Vault Backfill, SERCO/ERRA-0454.

Heyes, D., Butcher, E. J., Borwick, J., Milodowski, A. E., Field, L. P., Kemp, S. J., Mounteney, I., Bernal, S. A., Corkhil, C. L., Hyatt, N. C., Provis, J.L., Black, L., 2015. Demonstration of carbonation of the NRVB, NNL(14)13296.

Hidalgo, A., Domingo, C., Garcia, C., Petit, S., Andrade, C., Alonso, C., 2008. Microstructural changes induced in Portland cement-based materials due to natural and supercritical carbonation. J. Mater. Science, 43, 3101-3111.

Hills, C. D., Sweeney, R. E. H., Buenfeld, N. R., 1999. Microstructural study of carbonated cement-solidified synthetic heavy metal waste. Waste Management 19, 325-331.

Hobbs, D.W., 2001. Concrete deterioration: causes, diagnosis, and minimising risk. Int. Mater. Rev. 46, 117-144.

Hoffmann, U., Stipp, S. L. S., 1998. Preliminary results on the behaviour of Ni(II) in the calcite-water system, Mineralogical Magazine 62A, 642-643.

Johannesson, B., Utgenannt, P., 2001. Microstructural changes caused by carbonation of cement mortar. Cem. Concr. Res. 31, 925-931.

Landis, E.N., Keane, D.T., 2010. X-ray microtomography. Mater. Charact. 61, 1305-1316.

Lange, L. C., Hills, C. D., Poole, A. B., 1996. The effect of accelerated carbonation on the properties of cement-solidified waste forms. Waste Management 16, 757-763.

Lange, L. C., Hills, C. D., Poole, A. B., 1997. Effect of carbonation on properties of blended and non-blended cement solidified waste forms. J. Hazard. Mater. 52, 193-212.

Lothenbach, B., Le Saout, G., Gallucci, E., Scrivener, K., 2008. Influence of limestone on the hydration of Portland cements. Cem. Concr. Res. 38, 848-860.

Matschei, T., Lothenbach, B., Glasser, F.P. 2007. The role of calcium carbonate in cement hydration. Cem. Concr. Res., 37, 551-558

Milodowski, A. E., Field, E., Butcher, A., Parkes, D., 2013. Preliminary petrographic and micropermeametry investigations of reacted cements from National Nuclear Laboratory experiments on Nirex Reference Vault Backfill (NRVB) cement carbonation. British Geological Survey Commissioned Report CR/13/027.

Morandeau, A., Thiéry, M., Dangla, P., 2014. Investigation of the carbonation mechanism of CH and CSH in terms of kinetics, microstructure changes and moisture properties. Cem. Concr. Res. 56, 153-170.

Nuclear Decommissioning Authority, 2010a. NDA/RWMD/033. Geological disposal, Near-field evolution status report.

Nuclear Decommissioning Authority, 2010b. NDA/RWMD/037. Geological disposal, Gas status report.

Nishikawa, T., Suzuki, K., Ito, S., 1992. Decomposition of synthesized ettringite by carbonation. Cem. Concr. Res. 22, 6-14.

Poonguzhali, A., Shaikh, H., Dayal, R.K., Khatak, H.S., 2008. Degradation mechanism and life estimation of civil structures – A review. Corros. Rev. 26, 215-294.

Poulsen, S. L., Jakobsen, H. J., Skibsted, J., 2010. Incorporation of phosphorus guest ions in the calcium silicate phases of Portland cement from 31P MAS NMR spectroscopy. Inorg. Chemistry 49, 5522-5529.

Provis, J. L., Myers, R. J., White, C. E., Rose, V., van Deventer, J., 2012. X-ray microtomography shows pore structure and tortuosity in alkali-activated binders. Cem. Concr. Res. 42, 855-864.

1189 Richardson, I. G., Skibsted, J., Black, L., Kirkpatrick, R. J., 2010. Characterisation of
1190 cement hydrate phases by TEM, NMR and Raman spectroscopy. Adv. Cem. Res. 22,
1191 233-248.
1192
1193 Rochelle, C. A., Milodowski, A. E., 2013. Carbonation of borehole seals: comparing
1194 evidence from short-term laboratory experiments and long-term natural analogues.
1195 Appl. Geochemistry 30, 161-177.
1196
1197 Shafique, M., Walton, J., Gutierrez, N., Smith, R., Tarquin, A., 1998. Influence of
1198 carbonation on leaching of cementitious wasteforms. J. Environmental Engineering
1199 124, 463-467.
1200
1201 Snyder, R. L., Bish, D. L., 1989. Quantitative analysis. In: D. L. Bish, J. E. Post,
1202 (editors), Modern Powder Diffraction, Reviews in Mineralogy, Volume 20,
1203 Mineralogical Society of America, USA, 101-144.
1204
1205 Sun, J., 2010. Carbonation Kinetics of Cementitious Materials Used in the Geological
1206 Disposal of Radioactive Waste, PhD thesis, University of London.
1207
1208 Thiery, M., Villain, G., Dangla, P., Platret, G., 2007. Investigation of the carbonation
1209 front shape on cementitious materials: Effects of chemical kinetics. Cem. Concr. Res.
1210 37, 1047-1058.
1211
1212 Villain, G., Thiery, M., Platret, G., 2007. Measurement methods of carbonation
1213 profiles in concrete: thermogravimetry, chemical analysis and gammadensimetry.
1214 Cem. Concr. Res. 37, 1182-1192.
1215
1216 Živica, V., Bajza, A., 2001. Acidic attack of cement based materials — a review: Part
1217 1. Principle of acidic attack. Constr. Build. Mater. 15, 331-340.
1218